The University of Texas at TYLER
The Graduate School

University of Texas at Tyler
Scholar Works at UT Tyler

Mechanical Engineering Theses | Mechanical Engineering

Fall 8-5-2015

Measured and Predicted Performance of a Photovoltaic Grid-Connected System in a Humid Subtropical Climate

Racquel Lovelace

Follow this and additional works at: https://scholarworks.uttyler.edu/me_grad

 Part of the Mechanical Engineering Commons

Recommended Citation

Lovelace, Racquel, "Measured and Predicted Performance of a Photovoltaic Grid-Connected System in a Humid Subtropical Climate" (2015). *Mechanical Engineering Theses.* Paper 3.
http://hdl.handle.net/10950/289

This Thesis is brought to you for free and open access by the Mechanical Engineering at Scholar Works at UT Tyler. It has been accepted for inclusion in Mechanical Engineering Theses by an authorized administrator of Scholar Works at UT Tyler. For more information, please contact tbianchi@uttyler.edu.

The University of Texas at TYLER
The Graduate School

MEASURED AND PREDICTED PERFORMANCE OF A PHOTOVOLTAIC GRID-CONNECTED SYSTEM IN A HUMID SUBTROPICAL CLIMATE

by

RACQUEL LOVELACE

A thesis submitted in partial fulfillment
of the requirements for the degree of
Masters of Science
Department of Mechanical Engineering

Fredericka Brown, Ph.D., Committee Chair

College of Engineering

The University of Texas at Tyler
July 2015

The University of Texas at Tyler
Tyler, Texas

This is to certify that the Master's Thesis of

RACQUEL LOVELACE

has been approved for the thesis requirement on
July 23rd 2015
for the Masters of Science degree

Approvals:

_____
Thesis Chair: Fredericka Brown, Ph.D.

_____
Member: Dominick Fazarro, Ph.D.

_____
Member: Harmonie Hawley, Ph.D.

_____
Chair, Department of Mechanical Engineering

_____
Dean, College of Engineering

Acknowledgements

The investigative effort presented in this paper has been completed in the frame of research work at the Department of Mechanical Engineering, University of Texas at Tyler, Texas for master's program. The author gratefully acknowledges Fredericka Brown for her support and guidance in the research work.

Table of Contents

List of Tables

List of Figures

Abstract

MEASURED AND PREDICTED PERFORMANCE OF A PHOTOVOLTAIC GRID-CONNECTED SYSTEM IN A HUMID SUBTROPICAL CLIMATE

Racquel Lovelace

Thesis Chair: Fredericka Brown, Ph.D.

The University of Texas at Tyler
July 2015

Solar energy is an alternative energy source that has the potential to provide energy for the very increasing global population. Photovoltaic modules are the means by which solar energy is collected. Photovoltaic modules convert sunlight into direct-current (DC) electricity which can then be converted to alternating current (AC) electricity and used in regular household systems.

This research aimed to determine the measured and predicted performance of a photovoltaic grid-connected system in a humid subtropical climate. Simulation and numerical models were used to determine the predicted performance of the system to be compared to the recorded data from the system. In addition, the research allowed for long term simulation analysis of the system under varying conditions and can assist with optimization of the photovoltaic system.

Chapter 1

Introduction and General Information

1.1 Models of PV Systems/Modules

As the global population increases along with the advancement of human development and technology, so does the increase in global energy demand. According to the US Energy Information Administration's 2013 report, the world energy consumption is expected to grow by 56% between 2010 and 2040, from 524 quadrillion British thermal units (Btu) to 820 quadrillion Btu (Figure 1) [1]. Through these projections, it was estimated that fossil fuels will continue to supply roughly 80% of the world energy through 2040 [1].

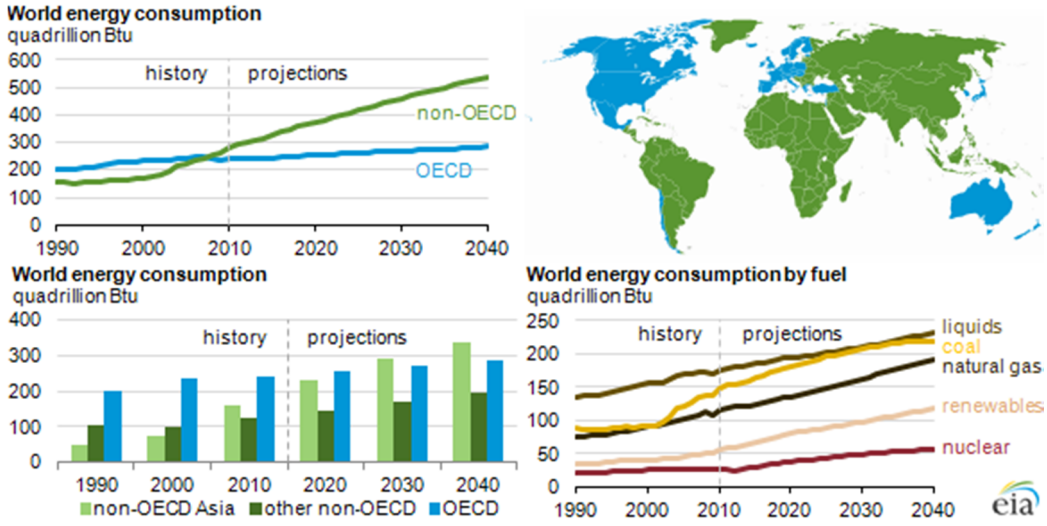

Figure 1. Energy Information Administration's projections for world energy consumption [1].

Fossil fuels are non-renewable resources with supplies that are drastically being depleted. It was calculated that the depletion time for oil, gas and coal was to be around 35, 37 and 107 years, respectively [2]. Though the accurate timing for fossil fuel depletion is an arguable topic among researchers and scientists, it is an inarguable fact that fossil fuels cannot last forever at the current usage rates. The increase in demand for energy coupled with the knowledge of depleting fossil fuels has led to an increase in demand for research into developing an alternative to using

fossil fuels. Renewable energy sources include biomass, hydropower, geothermal, nuclear, solar, wind and marine energies [3]. Each source has advantages and disadvantages to being an alternative to fossil fuels; however the most viable alternative currently is solar energy.

Solar energy has been the focus of copious research due to its many advantages as a renewable energy source. Solar energy has advantages over its renewable energy counterparts of biomass, hydropower, geothermal, nuclear, wind and marine. The key advantages of solar energy can be highlighted by the following characteristics: 1) the direct use of heat in the absorption of solar radiation, 2) absence of moving parts, 3) low maintenance cost once installed, 4) ability to easily scale the input power source to generate desired output, 5) long effective life, 6) high reliability, 7) rapid responses to weather/environment changes, 8) high power handling capabilities and 9) availability to be utilized across the globe [4]. Adversely, solar energy continues to have limiting major factors to its wide industrial and commercial use. Improved performance and efficiency for overall systems (such as photovoltaic systems as the main topic of this research) and energy storage (for use in the absence of solar radiation) are needed before this energy source can be effective in providing for the global population.

Photovoltaic (PV) modules are solid-state semiconductor devices that convert sunlight into direct-current (DC) electricity [5]. PV production has been doubling every two years, increasing by an average of 48% each year since 2002, making it the world's fastest-growing energy technology [6]. PV systems depend on a variety of factors including but not limited to: weather, irradiation levels, temperature, and efficiencies in all components of the system. Various methods have been developed to determine the maximum power output of these photovoltaic systems to improve overall efficiency. These methods have included the use of numerical, experimental and analytical models of the photovoltaic system while taking into account losses

due to dirt and dust, angularity, differences with the nominal power, mismatch, monitoring errors of the maximum peak, ohmic losses in cabling and losses due to shading. Experimental and simulation models are also widely used in the evaluation of photovoltaic systems.

This research aimed to determine the measured and predicted performance of a photovoltaic grid connected system in a humid subtropical climate. The system used in the study was connected to the Texas Allergy, Indoor Environment, and Energy Institute (TxAIRE) House 2, located on the University of Texas at Tyler campus. Simulation and numerical models were used to determine the predicted performance of the system to be compared to the experimental data received from the TxAIRE House 2. This research allowed for long term simulation analysis of the system under varying conditions and can assist with the optimization of the photovoltaic system.

Chapter 2

Literature Review

Though the efficiency of PV systems has increased over the past 10 years as new research and development projects continue, average efficiencies have ranged between a low 15% - 20% [7]. Due to this, vast amounts of research have been conducted to improve the way PV system outputs and efficiencies are calculated. Developed performance models help with improving the overall performance of the system by being able to predict the performance under various conditions using differing configurations to determine the optimum system. This section will review various methods to determine the performance of PV systems using numerical methods.

2.1 Models of PV Systems/Modules

In 1998, the International Electrotechnical Commission (IEC) published a standard for analyzing the electrical performance of the PV system [8]. The following equation was developed to calculate the amount of annual energy produced for grid-connected photovoltaic power systems.

$$P_{annual} = \frac{G_a(\beta, \alpha) \cdot P_{peak} \cdot PR}{G_{STC}} \quad (1)$$

G_a (β,α) is the annual solar radiation on the generator surface, P_{peak} is the installed photovoltaic peak power, PR is the "Performance Ratio" which is the annual yield of the facility and G_{STC} is the solar irradiance under standard test conditions. Standard test conditions (STC) are defined as an incident irradiance of 1 kW/m^2, temperature of the photovoltaic cell of 25 °C, and AM_{STC} 1.5G standard spectrum. The performance ratio was calculated using experimental data and was dependent on numerous factors such as solar radiation availability, climate, orientation and tilt of the surface, quality of the components and design of the system, among

others. The performance ratio in this equation was the main component for determining the overall electrical performance of the PV system. Other methods have been developed to determine this output, such as the equation for PR described by Almonacid et al [9]. Almonacid et al. explain that the PR was the efficiency of the photovoltaic generator and was calculated as one minus the sum of the losses incurred in the system, explained in section 5, and shown by Equation (2).

$$PR = (1 - \sum Li) \tag{2}$$

Another equation to express the performance ratio was used by T. Erge et al. [10] as shown by Equation (3).

$$PR = \frac{P_{INV}}{G \times \eta_{STC}} \tag{3}$$

P_{INV} is the AC-energy output from the inverter, G is the total solar energy on the array plane and η_{STC} is the efficiency of the array at standard test conditions. This method to calculate the PR required experimental data for the solar irradiance and the power output of the inverter to be used for calculations versus the previous method in which only the calculated values of the losses were needed. This method would yield a more accurate result though timing would be a factor in the amount of time needed to obtain the result as the experimental data would need to be collected.

Other calculations for power do not take into account a PR factor as those mentioned previously. T. Huld et al. [11] developed a model for power output that takes into account only module temperature and the solar irradiance as expressed by Equation (4). This was different than the IEC in that it did not take into account the PR.

$$P(G,T) = P_{STC} \cdot \frac{G}{G_{STC}} \cdot \eta_{rel}(G',T') \quad (4)$$

where P_{STC} is the power at standard test conditions of G_{STC} = 1 kW/m^2 and T_{STC} = 25 °C. This equation used the instantaneous/hourly relative efficiency as given by Equation (5).

$$\eta_{rel}(G',T') = 1 + k_1 lnG' + k_2[lnG']^2 + T'(k_3 + k_4 lnG' + k_5[lnG']^2) + k_6 T'^2 \quad (5)$$

$$G' \equiv G/G_{STC} \quad (6)$$

$$T' \equiv T - T_{STC} \quad (7)$$

$$T = T_a + c_T G \quad (8)$$

The coefficents k1-k6 were found by fitting the model to experimental data. The instantaneous efficiency depends on the irradiance and module temperature. G' and T' are normalzed parameters to the STC values and are expressed by Equations (6) and (7) while the module temperature was estimated using Equation (8). These equations allow for energy yield calculations to take place under varying climatic conditions over a large geographical area [11].

The equations expressed so far were basic equations to determine power performance and efficiency, however there exist advanced models to determine power output, inverter efficiency and system effieciency. The following models use single-diode, two-diode and four and five parameter models to determine the power performance of a photovoltaic sytem.

2.1.1 Single-diode

The following models were developed using the single-diode model. The single-diode model assumes that one lumped diode mechanism was sufficient to describe the characteristics of the PV cell [12]. The term "lumped" refers to the type of approximation being made; in this case it was assumed that the circuit parameters such as resistance and capacitance can be taken as fixed quantities. The term "single mechanism" refers to the degree of approximation that was used to model the photovoltaic cell.

H. Tian et al. [12] used the following Equations (9) and (10), derived from the single-diode model, to calculate the maximum power point current and voltage at any operating condition. A similar method was described by M. Fuentes et al. [13] as the approximate maximum power point (AMPP) method and was evaluated as having a root mean square error (RMSE) and mean bias error (MBE) to be smaller than 2% and 4%, respectively. The RMSE was calculated as the root mean square error in maximum power prediction as a percentage of the average measured value of maximum power. Another similar method was also described by P Mohanty et al. [14] and M. Paulescu et al. [15] as a way to calculate the output current.

$$I_{mp} = N_P I_{ph} - N_P I_0 \left[\exp\left(\frac{q\left(V_{mp} + I_{mp}\frac{N_S}{N_P}R_S\right)}{N_S nkT} \right) - 1 \right] - \frac{V_{mp} + I_{mp}\frac{N_S}{N_P}R_S}{\frac{N_S}{N_P}R_P} \tag{9}$$

$$\frac{I_{mp}}{V_{mp}} = \frac{\frac{qN_P I_0}{N_S nkT}\exp\left(\frac{q\left(V_{mp} + I_{mp}\frac{N_S}{N_P}R_S\right)}{N_S nkT} \right) + \frac{1}{\frac{N_S}{N_P}R_P}}{1 + \frac{qI_0 R_S}{nkT}\exp\left(\frac{q\left(V_{mp} + I_{mp}\frac{N_S}{N_P}R_S\right)}{N_S nkT} \right) + \frac{R_S}{R_P}} \tag{10}$$

M. Paulescu et al. developed the single-diode equations further to be able to calculate the I-V curve outside of the standard test conditions based on: solar irradiance, ambient temperature, the cleanliness degree of module surface (the cleanliness degree was calculated using experimental models and is outlined in Table 1) and the ageing degree of the PV module. Equations (11) – (12) show the calculations for the modified I-V curve outside standard test conditions.

$$G_{ef} = \tau_C G \tag{11}$$

$$I_{ph}(G,T) = I_{ph,STC}(G_{STC})[1 + \alpha_1(T - T_{STC})]\frac{G_{ef}}{G_{STC}} \tag{12}$$

$$I_0(G,T) = I_{ph}(G,T)\exp\left(-\frac{eV_{OC,STC}[1+\alpha_V(T-T_{STC})]}{nkT}\right) \quad (13)$$

α_1 and α_v are the coefficients of variation with temperature of the short circuit current and the open circuit voltage, respectively. These equations are functions of solar irradiance and temperature and are dependent on these two factors as well as the open circuit voltage at STC, Boltzmann's constant and the diode ideality factor. The diode ideality factor is a measure of how closely the diode follows the ideal diode equation; for the equations discussed in this paper the ideality factor is assumed to be one unless otherwise defined. The values of I_0, I_{ph}, n and R_s were introduced in the solar cell I-V characteristic equation so that it may be used for conditions other than the standard test conditions [15].

Table 1. The cleanliness coefficient.

Cleanliness	**Perfect**	**Proper**	**Medium**	**Low**
$\boldsymbol{\tau_C}$	1.00	0.98	0.96	0.92

Another method, derived from the single-diode model, to evaluate the performance of a PV system would be to use data supplied by the manufacturer of the solar panels. A model presented by De Soto [16] used a one-time calculation of the following five parameters: n, I_o, I_{ph}, R_s, and R_p at standard test conditions. These values can then be used within the model to calculate the parameters at different operating conditions. The power supplied by the PV system is determined by multiplying the current and voltage. Equations (14) and (15) depict the relationship between current and voltage at a fixed cell temperature and solar irradiation. The five parameters were used to determine the current and voltage.

$$I = I_{ph} - I_0\left[e^{\frac{V+IR_S}{n}} - 1\right] - \frac{V+IR_S}{R_P} \quad (14)$$

$$n \equiv \frac{N_S n_1 kT}{q} \quad (15)$$

where n in this case is the modified ideality factor and n_1 is the usual ideality factor assumed to be one. These equations were used in conjunction with the three known I-V pairs at standard test conditions which were substituted in to result in further equations to predict power. De Soto's method has been referenced in many articles as a basis for further research in developing numerical models to determine predicted power of a PV system. Similar models were used by Zekiye Erdem and M. Bilgehan Erdem [17] in distance education (i.e. online classes/study) and by A. Chouder et al. [18].

Kumari and Babu [19] developed equations for the I-V curves depending on changing temperature and solar irradiation levels for the PV system, though ultimately the values in question were still voltage and current. Equations (16) – (23) show the equations used to determine current and voltage as determined by Kumari and Babu.

$$C_{TV} = 1 + \beta_T(T_a - T_x) \tag{16}$$

$$C_{TI} = 1 + \frac{\gamma t}{G_{STC}}(T_x - T_a) \tag{17}$$

$$C_{sV} = 1 + \beta_T \alpha_S(G_x - G_{STC}) \tag{18}$$

$$C_{sI} = 1 + \frac{1}{G_{STC}}(G_X - G_{STC}) \tag{19}$$

$$V_{cx} = C_{TV} C_{sV} V_{STC} \tag{20}$$

$$I_{phx} = C_{TI} C_{SI} I_{ph,STC} \tag{21}$$

$$P = V_{STC}\left(I_{ph,STC} - I_a \times \exp\left(\frac{q}{kT} V_{STC} - I_0\right)\right) \tag{22}$$

$$I = I_{ph,STC} - I_0 \times \exp\left(\frac{q}{kT} V_{STC} - I_0\right) \tag{23}$$

These equations are functions of temperature and irradiance which are dependent on voltage at STC, photocurrent at STC and the reverse saturation current of the diode. De Soto and Kumari

both have employed the five parameter model which takes into account five parameters from the manufacturing data sheet of the PV panels, though both still derived from the single-diode model. Other models, such as those derived from the two-diode model, can be used as well.

2.1.2 Two-diode

Though it is more common to use the single-diode model for its simplicity, the two-diode model offers a model with greater accuracy to calculate the I-V curves as expressed by Equation (24) [20, 21]. The issue with using the two-diode model is that it requires the computation of seven parameters (I_{ph}, I_{O1}, I_{O2}, R_P, R_S, a_1 and a_2) while the single-diode model only requires four or five parameters.

$$I = I_{ph} - I_{01}\left[\exp\left(\frac{V + IR_S}{a_1 V_{T1}}\right) - 1\right] - I_{02}\left[\exp\left(\frac{V + IR_S}{a_2 V_{T2}}\right) - 1\right] - \left(\frac{V + IR_S}{R_P}\right) \quad (24)$$

where I_{01} and I_{02} are the reverse saturation currents of diode 1 and diode 2, respectively. Variables a_1 and a_2 represent the diffusion and recombination current component, respectively. It is widely assumed, though not always true, that $a_1 = 1$ and $a_2 = 2$. The parameters in this equation are functions of temperature, current and solar irradiance.

Research has been performed to simplify the two-diode model as well as decrease the computation time for this model; however the research has not been conclusive enough to outweigh the benefits of the simpler and faster single-diode model which offers sufficient accuracy.

2.1.3 Four parameter model

From the single-diode model, either a four or five parameter model can be developed to determine the I-V relationship. Equation (25) shows the relationship between current and voltage using the four parameter model [22]; others have used similar four parameter models for determining the I-V curve [23, 24, 25, 26].

$$I = I_{ph} - I_D = I_{ph} - I_O \left[\exp\left(\frac{V + IR_S}{n}\right) - 1\right] \quad (25)$$

The four parameters are functions of temperature, load current and/or solar irradiance. Most of the data to determine the four parameters can be obtained from the manufacturer data sheets similar to the De Soto model, except for the temperature and irradiance levels which must either be assumed or collected from weather data.

T. Khatib et al. [27] used the four parameter model to characterize a photovoltaic system in a grid connected PV system located in Malaysia. T. Khatib et al. determined that the four parameter model yielded accurate results compared to the experimental data recorded on the photovoltaic system.

2.1.4 Five parameter model

The five parameter model can more accurately calculate the power output; however there is the added complexity of another parameter calculation. A method of determining power output of a PV system using a five parameter model is Equation (26) for the I-V relationship curve [28].

$$I = N_p I_{ph} - N_p I_0 \left[\exp\left(\frac{qV}{kTnN_s} - 1\right)\right] \quad (26)$$

The typical I-V relationship curve contains the following variables, other than current (I) and voltage (V): N_S is the number of cells connected in series, N_p is the number of modules connected in parallel, q is the charge of an electron, k is the Boltzmann's constant, n is the ideality factor, I_0 is the cell reverse saturation current, and T is the cell temperature.

T. Ma et al. [29] employed the following Equations (27) – (31) in Matlab to simultaneously calculate the five unknown parameters (I_{ph}, I_0, V_t, R_s and R_p) using five equations. Similar equations to extract either the four or five parameters, depending on the model employed, the following researchers have used similar equations to those used by T. Ma et al. [26, 30, 31, 32,

33, 34, 35]. M.J.M. Pathak et al. [36] also employed the used of the five parameter model to optimize limited solar roof access.

i. For an open circuit under the STC, i.e. $I = 0$ and $V = V_{oc}$

$$0 = N_p I_{ph} - N_p I_0 \left(e^{\frac{V_{oc}}{N_S V_t}} - 1 \right) - \frac{N_p}{N_s} \frac{V_{oc}}{R_p} \tag{27}$$

ii. For a short circuit under the STC, i.e. $V = 0$ and $I = I_{sc}$

$$I_{sc} = N_p I_{ph} - N_p I_0 \left(e^{\frac{V_{oc}}{N_S V_t}} - 1 \right) - \frac{I_{sc} R_s}{R_p} \tag{28}$$

iii. The maximum power point under STC, i.e. $I = I_m$ and $V = V_{mp}$

$$I_{mp} = N_p I_{ph} - N_p I_0 \left(e^{\frac{V_{oc}}{N_S V_t}} - 1 \right) - N_p \frac{\frac{V_{mp}}{N_s} + \frac{I_{mp}}{N_p} R_s}{R_p} \tag{29}$$

iv. The derivative of the power with respect to voltage is equal to zero at the maximum power point,

$$\frac{I_{mp}}{V_{mp}} = -\frac{dI}{dV}\bigg|_{\substack{V = V_{mp} \\ I = I_{mp}}} \tag{30}$$

v. The fifth equation is established form the derivative of the current with the voltage at the short circuit point,

$$-\frac{dI}{dV}\bigg|_{\substack{V = V_{mp} \\ I = I_{mp}}} = \frac{\frac{\partial f(I,V)}{\partial V}}{1 - \frac{\partial f(I,V)}{\partial I}}\bigg|_{\substack{V = 0 \\ I = I_{sc}}} = \frac{-\frac{N_p}{N_s V_t} I_0 e^{\frac{I_{sc}\frac{N_s}{N_p} R_s}{N_s V_t}} - \frac{1}{\frac{N_s}{N_p} R_p}}{1 + \frac{R_s}{V_t} I_0 e^{\frac{I_{sc}\frac{N_s}{N_p} R_s}{N_s V_t}} + \frac{R_s}{R_p}} = -\frac{1}{R_p} \tag{31}$$

The following equations were then used to obtain the I-V curves of the PV cell/module/array under any general operating conditions [29].

$$I_{ph}(G,T) = I_{ph}[1 + \alpha_{I_{sc}}(T - T_{STC})]\frac{G}{G_{STC}} \tag{32}$$

$$I_0 = AT^3 \exp\left(\frac{-E_g}{nkT}\right) \tag{33}$$

$$V_t(T) = V_t\frac{T}{T_{STC}} \tag{34}$$

$$R_p(G) = \frac{R_p}{G/G_{STC}} \tag{35}$$

An improved version of the five parameter model was proposed by V. Lo Brano et al. [37] and was expressed by Equation (36).

$$I(\alpha_G,T) = \alpha_G I_{ph}(T) - I_0(\alpha_G,T)\left(e^{\frac{\alpha_G[V+KI(T-T_{STC})]+IR_s}{\alpha_G nT}} - 1\right) - \frac{\alpha_G[V + KI(T - T_{STC})] + IR_s}{R_P} \tag{36}$$

$$K = \frac{V_{mp} - V_{mp,STC}}{I_{mp,STC}(T - T_{STC})} \tag{37}$$

α_G is the ratio between the current irradiance and the irradiance at standard test conditions and K is the thermal correction factor which is used to slide the I-V curve to better fit the characteristics issued by the manufacturer. This equation allows for the computation of the I-V curve for any conditions of operating temperature and solar irradiance using only data that is commonly provided by manufacturers.

As stated, there are several different methods to employ when determining photovoltaic output power. The four parameter model derived from the single-diode model is a compromise between accuracy and simplicity. The accuracy is enough that the method is widely used among research and development in solar energy. The five parameter model is also widely used and offers a greater accuracy than the four parameter model, though computation is lengthy. Methods

involving the two-diode model are not widely used because of its complexity and the number of parameters needed, though currently it is the most accurate of the models discussed. An in depth look into the factors that contribute to the performance of the photovoltaic system are discussed in the following sections.

2.2 Calculating Cell Temperature

An important factor in determining photovoltaic system performance is temperature of the cells. Cell temperature is difficult to measure as the cells are tightly enclosed to protect against the elements. L.M. Ayompe et al. [38] reviewed several models to calculate PV module temperature and determined, through experimental data, that Equations (38) and (39) gave the lowest percent mean absolute error of 7.3% and 7.1%, respectively.

$$T = a + bG + cT_a + dV_w \tag{38}$$

$$T = T_a + \frac{G}{G_{STC}}[aV_w^2 + bV_w + c] \tag{39}$$

where values of the system-specific regression coefficients *a, b, c* and *d* are determined using measured temperature data.

A similar method to calculating cell temperature was expressed by Equation (40) [39].

$$T = T_a + (NOCT - 20°C)\frac{G}{800} \tag{40}$$

This was a simple equation that takes into account ambient temperature (T_a), the irradiance (G) and the normal operating cell temperature (*NOCT*) to predict the temperature of the effective modules. Normal operating cell temperature ratings assume the following: incident irradiance of 800 W/m^2, average 20°C ambient temperature, an average wind speed of 1 m/s with the back side of the solar panel open to the breeze which yields an average cell temperature of about 48°C.

2.3 Calculating Incident Global Solar Irradiance

Other than temperature, incident solar irradiance is another large factor in determining photovoltaic system performance. This factor can be divided into three components: the beam component from direct irradiation of the tilted surface, the diffuse component and a reflected component. C. Demain et al. [40] reviewed 14 different models to calculate the incident solar irradiance and determined, using mean bias error (MBE) and root mean square error (RMSE), that the Bugler model has the smallest error in calculating irradiance expressed by Equation (41).

$$R_d = \frac{1}{2}(1 + cos\beta) + 0.05\frac{B_\beta}{D}\left(cos\theta_i - \frac{1}{cos\theta_Z}\left(\frac{1 + cos\beta}{2}\right)\right) \quad (41)$$

with R_d being the ratio of diffuse radiation on the tilted surface with respect to that of the horizontal plane, B_β as the beam component from direct irradiation, β as the surface tilt angle with respect to the horizontal plane, θ_i as the incidence angle of beam irradiation and θ_z as the solar zenital angle.

2.4 Loss factors in a Grid-Connected System

The equations and methods discussed so far are a good starting point when determining output of a PV system, however to get accurate performance output data, loss factors have to be taken into account [41, 42, 43]. The following loss factors are explored in this section: losses due to dirt and dust, angular losses, losses due to differences with the nominal power, mismatch losses, temperature losses, losses due to monitoring errors of the maximum peak, ohmic losses in cabling, and losses due to shading.

2.4.1 Losses due to dirt and dust

An important factor to take into account when determining power output is the effect dust has on PV systems. Studies of Hottel and Woertz [44] in Boston, Massachusetts showed an average of 1% loss of incident solar irradiation due to the amount of dust accumulating on a glass plate with a tilt angle of 30° and a maximum degradation of 4.7% during the test period of three months. Multiple studies referenced in [44] performed in the northeastern United States have yielded similar results from 1% to 5% loss of incident solar irradiation. The areas in question for Hottel and Woertz's study have frequent precipitation and very low dust quantities in the atmosphere which should be considered when accounting for dust in solar panel performance in various climates and environments.

Studies performed by El-Shobokshy and Hussein [44] have produced the three key factors that contribute to PV performance degradation in terms of dust: the chemical composition of the dust material, the size of the dust particles, and the density of the dust on the panel surface (which is dependent on the first two factors). El-Shobokshy and Hussein were able to determine through lab testing that finer dust particles had a greater effect on the performance of PV cells than coarser dust.

Mulcue-Nieto [8] used a standard for calculating the amount of affect that dust has on the solar panels using the values in Table 2 and using Equation (42).

Table 2. Usual values of normal incidence loss due to dirt on the modules.

Degree of dirt	**$T_{dirt}(0)/T_{clean}(0)$**	**Losses (%)**
None	1	0
Low	0.98	2
Medium	0.97	3
High	0.92	8

$$L_{dirtiness} = 1 - \frac{T_{dirt}(0)}{T_{clean}(0)} \quad (42)$$

$T_{dirt}(0)$ is the transmittance of the normal incident light when the surface is covered with dust and $T_{clean}(0)$ is the same value when the surface is clean. This allowed for a simple way to take into account the effects of dirt into the overall PV performance. Experimental data has shown that typical loss due to dirt and dust was a factor of 0.95 [45].

2.4.2 Angular losses

Angular losses refer to the effect of the tilt angle as well as the orientation of the panels with respect to the South. One method to determine angular losses used the Martin-Ruiz [8] model. This model used values of direct, circumsolar diffuse (radiation coming from the direct beam from the sun and the area in the sky around the sun), isotropic diffuse (the radiation coming from the entire sky dome) and reflected radiation to determine the global irradiance. The global irradiance was calculated for every day of the year and was compared to the value in the case of the total absence of angular losses.

Martin-Ruiz's model was based on theoretical and experimental results. Equation (43) was Martin-Ruiz's model for the instantaneous/hourly angular losses factor [46, 47].

$$L_{ANG}(\theta_S) = 1 - \frac{1 - \exp(-\frac{cos\theta_s}{a_r})}{1 - \exp(-\frac{1}{a_r})} \quad (43)$$

θ_s represents the irradiance angle of incidence and a_r is the angular losses coefficient. Though Martin-Ruiz's method to calculate angular losses was a comprehensive approach, it was not one that was commonly applied for its complexity. The parameters required are not supplied by

module manufacturers and are difficult to establish and as far as PV plants are concerned, the input data was not commonly available.

2.4.3 Losses due to differences with the nominal power

The data supplied by the manufacturers of PV modules was data achieved under standard test conditions. These conditions were defined as an incident irradiance of 1 kW/m^2, temperature of the photovoltaic cell of 25 °C, and AM (air mass) 1.5G standard spectrum. The standard test conditions can not apply to every situation or environment, therefore losses due to a difference between the real power and the nominal power as stated by the manufacturer can occur [8].

Recent studies have shown an increase in accuracy between real power and nominal power, though inaccuracies still occur [8]. Mulcue-Nieto used Equation (44) to express the losses due to the inaccuracies.

$$L_{rating} = 1 - \frac{1}{Num\_mods} \sum_{i=1}^{Num\_mods} \frac{P_{real,i}}{P_{STC}} \quad (44)$$

Where real power ($P_{real,i}$) represents the real power of the i-th module. Studies have shown that the losses due to differences with the power under standard test conditions can be estimated as being equal to 5% as a maximum [8].

2.4.4 Mismatch losses

Mismatch losses occur when the sum of the individual power does not equal the total power of the system. This can be caused by: manufacturer's tolerances, degradation of the anti-reflective coating, discoloration of the housing material, degradation caused by light, hot points and the mechanical breaking of the cell structure [8]. Estimating the loss due to mismatch was not commonly performed and was usually calculated with experimental data and methods for

doing so were expressed in [48, 49]. Experimental data has shown that typical loss due to mismatch was a factor of 0.98 [45].

2.4.5 Temperature losses

Temperature losses due to convection and radiation can be calculated in several ways. Skoplaki and Palyvos [50] determined *T* (cell/module operating temperature) using Equation (45).

$$T = T_a + \left(\frac{G}{G_{NOCT}}\right)\left(\frac{U_{L,NOCT}}{U_L}\right)\left(T_{NOCT} - T_{a,NOCT}\right)\left[1 - \left(\frac{\eta}{\tau\alpha}\right)\right] \quad (45)$$

$U_{L,NOCT}$ is the thermal loss coefficient at normal operating cell temperature conditions, U_L the thermal loss coefficient, τ the transmittance of glazing and α is the solar absorptance. However, this equation used η which is itself a function of *T* and therefore an implicit model. Another explicit equation can therefore be used to determine the temperature *T* using Equation (46),

$$T = T_a + kG \quad (46)$$

Though in this linear expression there was no account for electrical load or wind. Another method to calculate temperature loss was to determine the difference between the real power and the hypothetical power produced if the cells were working at 25 °C (standard test condition). This gives the Equation (47) [8].

$$L_{temperature,ins} = -\gamma(T_i - 25) \quad (47)$$

γ is the variation coefficient of the power peak with the temperature.

2.4.6 Losses due to monitoring errors of the maximum peak power

Losses due to monitoring errors of the power maximum peak occurred when the inverter was not working correctly with the generator in the I-V curve and was not working at optimal working points. Losses then occurred due to power being generated that was lower than expected. The Spanish Centre for Technological, Environmental and Energy Research published

results showing a range of 4% and 6% of loss due to monitoring errors for clear days and partially clouded days, respectively [8].

2.4.7 Ohmic losses in the cabling

Losses due to cabling can be calculated using Equation (48) [8].

$$L_{ohmic} = \frac{\sum_{i=1}^{Num\_cables} \int_{\tau} I_l \cdot R_i^2 \cdot dt}{\int_{\tau} P_{max} dt} \quad (48)$$

This takes into account the number of cables and the amount of current that passes through the last cable with a certain resistance.

Another method was expressed using the following Equation (49) [51],

$$L_{i,ohmic} = I_a^2 \cdot R \quad (49)$$

The cable resistance was multiplied with the square of the 10 minute averaged DC-array current. The yearly losses can then be calculated by summing all power losses during the year [51]. Experimental data has shown that typical loss due to ohmic losses in cabling was a factor of 0.98 [45].

2.4.8 Losses due to shading

PV systems obtain all of their energy from the sun; therefore losses may occur if the PV panels are shaded. This loss depends on sun position as well as position of the PV panels in relation to possible obstructions (e.g. buildings, trees). This loss can be calculated by taking the sum of the multiplication of the area covered by the irradiance percentage of that region as shown in Equation (50) [8].

$$L_{shading} = \frac{1}{100} \sum_{i=1}^{Num\_mods} A_{obstacles} \cdot G_P \quad (50)$$

This loss can be difficult to determine as it can change throughout the day depending on the position of the sun in relation to the panels and any obstructions. Another method would be to use geographic coordinates and express the sun's position in the sky in terms of solar altitude above the horizontal plane and solar azimuth measured from the South [52]. This would allow a calculation using the geometrical parameters of the shading surfaces and the solar angles to determine the loss due to shading. Experimental data has shown that typical loss due to shading was a factor of 1.00 [45].

Shading losses can also be determined using photographic methods. One such software developed used photographs taken at the perspective of the horizon and required only measurements of three angles for each photograph [52]. Software can then use information from the picture and allow one to draw daily solar paths directly on the photograph and display how obstructions hinder the performance of a PV system.

Yoon et al. [53] developed a photographical method to predict solar irradiation on an inclined surface by combining the following solar irradiation models: the isotropic sky model (the simplest model which only takes into account the isotropic diffuse radiation), the Hay-Davies model (builds off the isotropic model and includes circumsolar diffuse radiation), the Reindl model (adds to the Hay-Davies model a horizon brightening parameter which is the solar radiation with source at the horizon), the Perez model (similar to the Reindl model, though more computationally intensive) and the Muneer model (similar to the Reindl model though developed two separate equations for a clear sky and an overcast sky) as well as the following ground reflectance models: the isotropic constant model (value for the ground reflectance was determined to be 0.2 after experimental data over four years was reviewed), the isotropic seasonal model (calculated the value for ground reflectance as a function of latitude), the

climatologically anisotropic model (the ground reflectance value is influenced by the zenith angle, period of the day and irrigation) and the semiphysical anisotropic model (the ground reflectance value was calculated using both direct and diffuse radiation).

Yoon et al. used the equations to determine the sky view factor (SVF) and the ground view factor (GVF) in existing solar irradiation models and modified them to take into account surrounding buildings and obstacles. Yoon et al. described using Holmer et al.'s software method to determine the SVF and GVF and the steps are shown below.

i. Import a scanned fisheye image (image taken using a fisheye lens which is an ultra wide-angle lens which creates wide panoramic or hemispherical images) to the IDRISI (a geographical information system and image processing program).
ii. Calculate the image center, radius and corner.
iii. Create the pixel weight image.
iv. Delimit the fisheye image.
v. Find the limit between sky and non-sky pixels.
vi. Assign the value 1 to all sky pixels, and 0 to all non-sky pixels.
vii. Multiply the images with each other.
viii. Sum the pixels, to calculate the SVF.

2.5 Efficiency Models

2.5.1 Photovoltaic system efficiency

Very simply the equation for efficiency can be expressed as the ratio of the output power to the solar irradiance per unit area of the PV modules [54]. However, more accurate equations have been developed to determine the efficiency. Hove [55] expressed the long-term average performance of photovoltaic systems using the following simple equations [55, 56].

$$\eta = \eta_{STC}\left[1 - 0.9\beta\frac{G_i}{G_{i,NOCT}}\left(T_{NOCT} - T_{a,NOCT}\right) - \beta\left(T_a - T_{STC}\right)\right] \quad (51)$$

$$P_{hourly} = \eta A G_i \quad (52)$$

These equations take into account the efficiency of the array at standard test conditions as well as the operating cell temperatures and cell temperatures at nominal operating conditions. These equations required measured data from operating photovoltaic systems but were useful in determining a general average performance without taking into account loss factors as mentioned in previous sections.

Dynamic models were developed because time-series analysis on hourly environmental data is only applicable to systems that respond slowly and linearly to changes in solar radiation [57]. Dynamic models allow for calculations to respond quicker to changes in the environment that the photovoltaic system is in.

K.H. Lam et al. [57] were able to develop a dynamic model for cell efficiency as expressed by Equation (53).

$$\eta = p\left[q\frac{G}{G_{STC}} + \left(\frac{G}{G_{STC}}\right)^m\right]\left[1 + r\frac{T}{T_{STC}} + s\frac{AM}{AM_{STC}}\right] \quad (53)$$

where G_{STC} = 1 kWm^2, T = 25 °C, AM_{STC} = 1.5 and the parameters *p, q, r, m* and *s* are coefficients as determined by applying the non-linear curve fitting for I-V curves acquired for the type of modules in use. This model was also used in experimental data at The University of Hong Kong by W. Durisch et al. [58].

2.5.2 Inverter conversion efficiency

The PV cells convert solar radiation into DC power and this power must be converted to AC power using an inverter, for grid-connected PV systems. The inverter is an integral part of a grid-connected PV system as it controls the power output that the grid sees [59].

There are several ways to determine the efficiency of the inverter. One such way took into account both the DC voltage and relative power, two factors that influence the behavior of the inverter and are regularly overlooked [59]. Equation (54) was a mathematical model that expressed the inverter efficiency as a function of relative power and DC input voltage.

$$\eta_{inv} = \frac{\left(\frac{P_{INV}}{P_{inv,STC}}\right)}{\left(\frac{P_{INV}}{P_{inv,STC}}\right) + \left(\left(K_{0_{V_{DCO}}} \pm S_0 V_{INV}\right) + \left(K_{1_{V_{DCO}}} \pm S_1 V_{INV}\right)\left(\frac{P_{INV}}{P_{inv,STC}}\right) + \left(K_{2_{V_{DCO}}} \pm S_2 V_{INV}\right)\right.} \quad (54)$$

Using this model, the efficiency can be determined at each point of DC voltage and relative power [59].

2.6 Uncertainty in PV Yield Predictions

Though copious amounts of research have been performed to create equations to calculate photovoltaic performance, it is known that certain factors and variables can have an effect on the effectiveness of the models. Due to this, equations to measure the uncertainty of a photovoltaic system have been created to use as a guideline when determining photovoltaic performance.

To model the uncertainty in long-term PV system performance information on the following factors is required: long-term average insolation, yearly and 20-year solar insolation variability, uncertainties introduced by the use of transposition (calculation of the incident irradiance on a tilted plan) models, module rating, degradation of PV modules, initial degradation, long-term degradation or ageing of the panels, availability, loss factors as mentioned in this paper.

Thevenard and Pelland [60] determined that the combined uncertainty σ_t in X can be calculated according to the rule of squares as expressed by Equation (55).

$$\frac{\sigma_t}{X} = \sqrt{\frac{\sigma_1^2}{X_1^2} + \frac{\sigma_2^2}{X_2^2} + \cdots + \frac{\sigma_N^2}{X_N^2}} \quad (55)$$

where (σ_n/X_n) is the loss factor of each loss in the system.

Statistical simulations performed by Thevenard and Pelland reveal that using the rule of squares and the values for each factor of uncertainty for a given case, the methodology discussed should be widely applicable.

2.7 Experimental Model of PV System

As mentioned, there are several methods and models to predict the performance of a photovoltaic system. However, some of the models do require input from experimental data and if resources are available it is recommended to compare predicted performance against experimental performance when using theoretical models.

Experimental photovoltaic systems use data acquisition systems (DAS) to monitor the output of the system. Equipment such as thermocouples to measure the back of the module temperature, pyranometers to measure the irradiance and laptops are commonly used to accurately measure data needed for the mentioned models.

Table 3 is a comprehensive list of characteristics that are used in the experimental setup as referenced by [13, 24, 30, 61, 62, 63, 64, 65, 66, 67, 68, 69].

Table 3. List of characteristics to be gathered for/from experimental setup.

Characteristic Name	**Unit**
Module Maximum Power in STC	W
Module Open Circuit Voltage in STC	V
Module Short Circuit Current in STC	A
Module Voltage at Maximum Power in STC	V
Module Current at Maximum Power in STC	A
Current/Temperature Coefficient	%/K
Voltage/Temperature Coefficient	%/K
Tilt Angle	Degree°
Ambient Temperature	°F
Wind Speed	MPH

Table 4 is a list of equipment that is commonly used when evaluating a photovoltaic system.

Table 4. List of common equipment to be used for experimental setup.

Equipment Name
Current-Voltage Curve Tracer (IVCT); ex. driven by LabVIEW
DataLogger
Reference Cells to Measure the Incident Global Irradiance
Thermocouples to Measure Back of Module Temperature

I-V curves are traced with the recorded data and the incident global irradiance is measured at each I-V point. With the data mentioned the performance parameters listed in Table 5 can be calculated [70]:

Table 5. List of parameters that can be calculated from IVCT.

Parameter Name
Total Energy Generated by the PV System
Final Yield
Performance Ratio
Capacity Factor
System Efficiency

Tables 3 – 5 listed above are a comprehensive list of values and equipment that can be used when evaluating a photovoltaic system; however it should be noted that not all of the items listed are necessary for the evaluation. Table 5 lists parameters calculated from a tracer listed in Table 4, though these are not needed for evaluating a photovoltaic system as these parameters can be calculated using the variables listed in Table 3, though it would be more accurate with the measured data.

2.8 Simulation Model of PV System

The use of simulation methods to predict photovoltaic performance has become more popular as software packages become more advanced to handle the various inputs and computations to generate the I-V curve. Commercial photovoltaic simulation software packages include, but are by no means limited to, options such as: TRNSYS, INSEL, Archelios, pvPlanner, PV*SOL, and

PVSYST. In order to use any one of the simulation packages mentioned, certain characteristics must be obtained either from the manufacturer data sheets of the various components of the photovoltaic system or from recorded data (e.g. ambient temperature). Table 6 is a comprehensive list of characteristics needed in the simulation setup as referenced by [29, 71, 72, 73, 74, 78].

Table 6. List of characteristics commonly used in the simulation setup.

Characteristic Name
Module Maximum Power in STC
Maximum Power Point Voltage at Reference Conditions
Maximum Power Point Current at Reference Conditions
Module Open Circuit Voltage at Reference Conditions
Module Short Circuit Current at Reference Conditions
Temperature at Reference Conditions
Irradiance at Reference Conditions
Module Voltage at Maximum Power in STC
Module Current at Maximum Power in STC
Current/Temperature Coefficient
Voltage/Temperature Coefficient
Tilt Angle
Ambient Temperature at NOCT Conditions
Module Temperature at NOCT Conditions
Insolation at NOCT Conditions
Power Tolerance
Module Efficiency
Transmittance-Absorptance Product at Normal Incidence
Semiconductor Band Gap
Wind Speed
Number of Cells in the Module Connected in Series
Number of Modules in Series in Each Sub-Array
Number of Sub-Arrays in Parallel
Individual Module Area
Azimuth of the Surface
Tracking Mode
Slope of the Surface
Orientation

In a grid connected system, an inverter is needed to convert the DC energy from the PV cells to AC. When simulating a grid connected photovoltaic system, the characteristics of the inverter are needed to help evaluate the actual amount of energy that is being supplied to the grid. Table 7 is a comprehensive list of characteristics that are generally monitored by inverter equipment that would be useful in the simulation setup as referenced [74].

Table 7. List of characteristics that are generally monitored by inverter equipment.

Characteristic Name
DC Current from PV Modules
Current from Each String
Inverter Input DC Voltage from PV Modules
Inverter Input DC Power from Generator
Inverter Output Total Energy
AC Current Injected into the Grid
Grid Current
Grid AC Phase Voltage
Grid Frequency
Grid Impedance
Inverter Operating Status
Error Code (Where Appropriate)
Number of Time that the Inverter Finds the MPP
Inverter Working Total Hours
Grid Injecting Total Hours
Total Connections to the Grid
Installation Boot-Up Number
Boot-Up Time
Inverter Operating Temperature
Isolation Resistance

Research has been performed to determine the calculative accuracy of commercial PV simulation software packages to compare against each other in their effectiveness. As discussed by Axaopoulos et al. [73] there are many simulation software packages available and five of them were compared to each other in terms of room mean square error (RSME), mean absolute

deviation (MAD) and mean absolute percentage error (MAPE). TRNSYS had shown to display a model efficiency of 99.7%, followed by Archelios with 5.1% error with MAPE, and PVSyst and PV*SOL with model efficiencies of about 92.5%.

Another topic of discussion that has come up in recent years is the ability to predict the future performance of PV systems using the methods mentioned and predicted weather data. The research was not as extensive, though various methods are discussed in the following section.

2.9 Future Performance Predictions

Few research papers were available on the predicted future performance of PV systems during the research for this study. Besides the characteristics of the PV modules, the performance of PV systems depends on the weather data. Forecasting weather parameters, such as radiation, can be difficult in that it is highly variable due to cloud cover and other factors. The research is still in its early stages; however methods include using climate change scenario predictions and other forecasting methodologies.

2.9.1 Future performance predictions using climate change scenarios

The North American Regional Climate Change Assessment Program (NARCCAP) is an international program that creates high resolution climate scenarios for North America using regional and global climate models and time-slice experiments. The models are run with a set of regional climate models driven by a set of atmosphere-ocean general circulation models. The driving atmosphere-ocean general circulation models are forced with the A2 SRES (Special Report on Emissions Scenarios, commissioned by the Intergovernmental Panel on Climate Change) emissions scenario in the future period. The emissions scenario takes into account predicted future world development in the 21st century including: economic development,

technological development, energy use, population change and land-use change to predict emission projections to incorporate into the climate change models.

As discussed by Shannon Patton [75] the NARCCAP results can be used to calculate the change in climate from the contemporary time period (1971 – 2000) to a future time period (2041 – 2070) for specific locations in North America. The change in climate characteristics (such as radiation, temperature and wind speed) can be used to predict future changes in the PV performance.

2.9.2 Future performance predictions using other methods

Other methods of solar forecasting include: regression models, artificial neural networks (ANNs), remote sensing, and numerical weather prediction models as discussed by Inman et al. [76] and Mathiesen et al. [77].

Early forecasting models for solar radiation included regression models. These models used data from long term averages and steady state values and extrapolated the data which resulted in static models that only described seasonal and diurnal changes. These models did not take into account the short term stochastic characteristics of solar radiation and assumed that individual observations of solar irradiance changed independently, though the opposite is true. Due to these deficiencies in this approach, new approaches had been researched. Improvements on regression models include remote models which use satellite data to predict solar radiation using measured solar radiation and its interaction with atmospheric components such as gasses and aerosols.

ANNs were developed to solve complex, non-linear, non-analytic, non-stationary, stochastic problems with little to no interferences with the program itself. ANNs have been increasingly used to forecast solar radiation from hours in the future to years. ANN programs can be created

and executed in programs such as Matlab, though they require knowledge into the structure of the various types of ANN programs available.

Numerical weather predictions (NWPs) were developed in the early 20th century; these predictions took into account the state of the atmosphere at an initial time and the physical laws which governed the transition of the atmosphere from one state to another to predict future weather conditions. NWPs are currently not able to solve physics associated with cloud formation which lead to the largest sources of error in a NWP based solar forecast.

2.10 Summary and Conclusions

This review aimed to examine and summarize the research and development that has been performed to develop comprehensive models to evaluate the overall performance of a grid-connected photovoltaic system. Four overarching types of models for PV systems were reviewed including: the five parameter model, the four parameter model, single-diode and two-diode models. The single-diode was a simpler version of the two-diode model and assumed a constant value for the ideality factor that was present in the two-diode model. This allowed for easier manipulation of the single-diode equation to develop the four or five parameter models. The four and five parameter models were characterized by the number of parameters that needed to be analytically calculated to determine the I-V curve. The five parameter model was more accurate, however it was more complex in that it required an extra equation to determine the fifth parameter as compared to the four parameter model. Most researchers seemed to use the single-diode model with either the four or five parameter model with accurate results based on experimental data.

In order to further improve the four or five parameter models, it has been determined that the two biggest factors in photovoltaic performance were cell temperature and the solar irradiance.

To create more accurate inputs for these two factors would be to greatly increase the overall accuracy of the photovoltaic performance model. Various equations to calculate the cell temperature and the irradiance were discussed. The cell temperature is a difficult factor to measure as the cell is completely encapsulated. Several cell temperature equations were researched and three equations were reviewed, one that offers a general equation for cell temperature and two others that offer error percentages of about 7% to calculate cell temperature as compared to experimental data. The irradiance factor similarly was researched and an equation that had the smallest error of 14 models was reviewed.

Loss factors are inherent in the system and must also be calculated and taken into account when determining performance. The losses discussed were: losses due to dirt and dust, angular losses, losses due to differences with the nominal power, mismatch losses, temperature losses, losses due to monitoring errors of the maximum peak, ohmic losses in cabling, and losses due to shading. Various ways to determine loss due to shading, such as the photographical method, were also discussed.

The efficiency models of the photovoltaic system were another way to determine the performance of the system based on comparing if the solar panels were 100% efficient at converting all energy received to the actual energy produced. Two models were discussed in calculating efficiency using the efficiency of the array at standard test conditions as well as the operating cell temperatures and cell temperatures at nominal operating conditions. Another way to determine the effectiveness of a model was to calculate the uncertainty in the yield predictions. The method reviewed uses statistical expression ‘rule of squares’ to determine the uncertainty.

The inputs and data needed to successfully and comprehensively determine the photovoltaic performance of experimental and simulation models were discussed. The inputs for the experimental model were all included in the list of inputs needed for the simulation model; however the simulation model needs a more extensive list to accurately simulate the photovoltaic system. Research has shown that the commercial software package TRNSYS, with the correct input data, yields highly accurate results compared to experiment and numerical data.

Lastly, various methods to determine future weather conditions were discussed including: NARCCAP climate change scenarios, regression models, ANNs, remote sensing, and numerical weather prediction models. Various levels of predictive success have been experienced with the methods discussed because of the stochastic characteristic of weather variables. Due to timing, the NARCCAP climate change scenario was decided on to predict future performance as the climate change had already been computed and was available for public use.

It was determined from the research provided that the single-diode, five-parameter model was an effective and accurate model to numerically predict the output energy of the PV system used by TxAIRE House 2. A simulation model using the TRNSYS software package was also determined to be useful in predicting output energy. The following sections detail the use of the predicted energy from both the numerical model and the simulation model compared to the actual experimental data collected from TxAIRE House 2 from the years 2012 and 2014, as well as a predictive model using the climate change data from NARCCAP.

Chapter 3

Research Methods and Procedures

The following chapter will discuss the layout of the PV system in question and the data collected during the years of 2012 through 2014 for the system. Various methods to determine the performance of a PV system have been discussed in the previous chapter. The most practical method for this study was chosen to be the one-diode, five-parameter model. This method can be used to determine PV performance algebraically and in simulation software as discussed in this chapter. As mentioned previously, the one-diode, five-parameter model offers a more accurate result of the PV performance than the four-parameter model (either one- or two-diode models). The two-diode, five-parameter model offers an even higher accuracy, however the complexity of the model due to the added variables that must be calculated makes it a less desirable model to use. The one-diode, five parameter model allows for easy calculations as all the inputs are determined from information given by the solar panel manufacturer data sheets. Therefore, this chapter will also detail the methods used and steps taken for De Soto's five-parameter model as well as the TRNSYS simulation software to determine PV output.

3.1 Description of the System

3.1.1 Solar panel equipment and set-up

The photovoltaic system used for this study was the system supplying the energy for TxAIRE House 2. TxAIRE House 2 is a Net-Zero Energy house as all the power is provided by the PV system. The house is air-tight with open-cell foam insulation, an unvented attic with an open-cell foam insulated roof deck, and vinyl-frame windows with double-pain, low-E glass. Every aspect of this house was designed to create an energy-efficient home.

The house has a photovoltaic grid-connected system, consisting of thirty-three SolarWorld® SunModule Plus™ polycrystalline 225 watt solar panels, rated at 7.4 kW. The performance standards under standard test conditions as well as the thermal characteristics as supplied by the manufacturer on the data sheet are shown in Table 8 and Table 9, respectively for the solar modules. The photovoltaic modules cover an area of 590 ft^2 and are situated 25 ft. away from the roofline of the house and are at a 55.8º angle as shown in Table 8 and Table 9.

Table 8. Performance under standard test conditions of 1000 W/m2, 25ºC, AM 1.5.

Characteristic	**Variable**	**SW 225**
Maximum power	P_{max}	225 Wp
Open circuit voltage	V_{oc}	36.8 V
Maximum power point voltage	V_{mpp}	29.5 V
Short circuit current	I_{sc}	8.17 A
Maximum power point current	I_{mpp}	7.63 A

Table 9. Thermal characteristics of solar panels.

Characteristic	**Parameter**
NOCT	45ºC
TC I_{sc}	0.034 %K
TC_{Voc}	-0.34 %K
TC P_{mpp}	-0.48 %K
Operating range	-40ºC to 90ºC

Figure 2. Back view of photovoltaic panels used in study.

Figure 3. Front view of photovoltaic panels used in study.

The solar panels used for the research are installed in three circuits of eleven modules per circuit for a total of 33 modules. The schematic shown in Figure 4 shows the solar panels as they are wired.

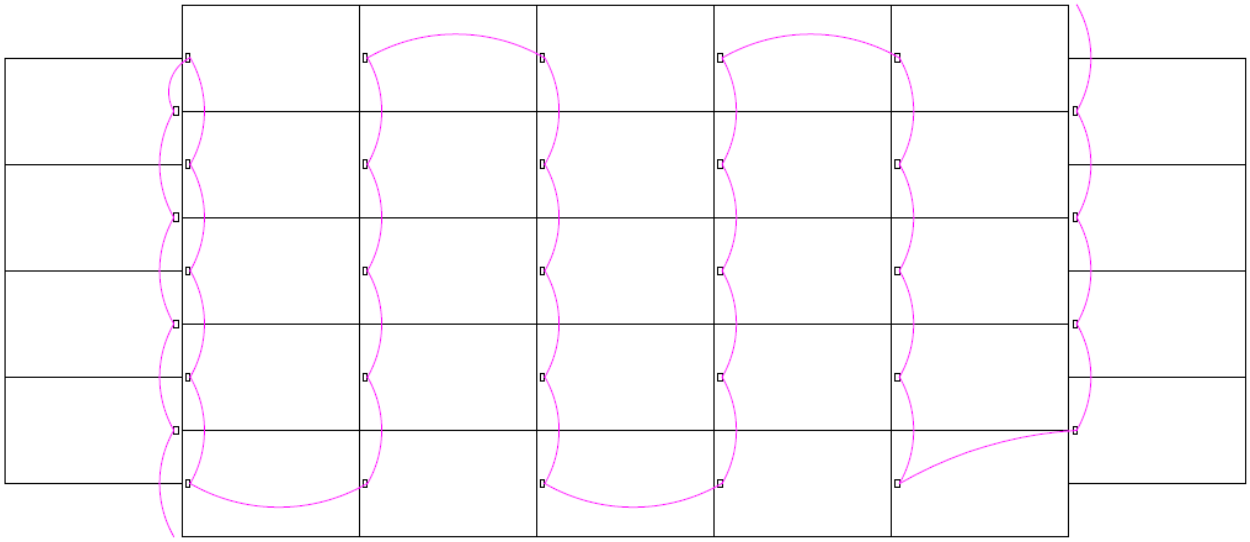

Figure 4. Schematic of solar panels wired together in series.

This array converts the solar radiation into DC electricity while an inverter unit is used to convert the DC electricity to AC so that it can be fed into the house's electrical system. The inverter unit in this system was manufactured by SMA Technology model #SB7000US.

3.1.2 Tyler, Texas climate and area

TxAIRE House 2 is located in Tyler, Texas which is classified as a humid subtropical climate with latitude 32.314592° N and longitude -95.2591° W at an altitude of 561 feet above sea level. Figure 5 shows the average high and low temperature and precipitation data for Tyler, TX as gathered by U.S. Climate data for each month from January 2012 – December 2014. The data shown in Figure 5 is not the exact data used in the simulations. The averages shown are used as a reference to show the average weather data in the area in which the photovoltaic system resides during the time that the archival data used was taken. The data shows that March and September of 2012, September and October of 2013, and June 2014 and October 2014 had the highest

amount of rain throughout the research time period. The data also shows that the months of July and August were the hottest months of the year for all three years reaching high temperatures of 94ºF for 2012, 95ºF for 2013 and 92ºF for 2014, with the coolest month being December for all years reaching low temperatures of 61ºF for 2012, 55ºF for 2013 and 59ºF for 2014.

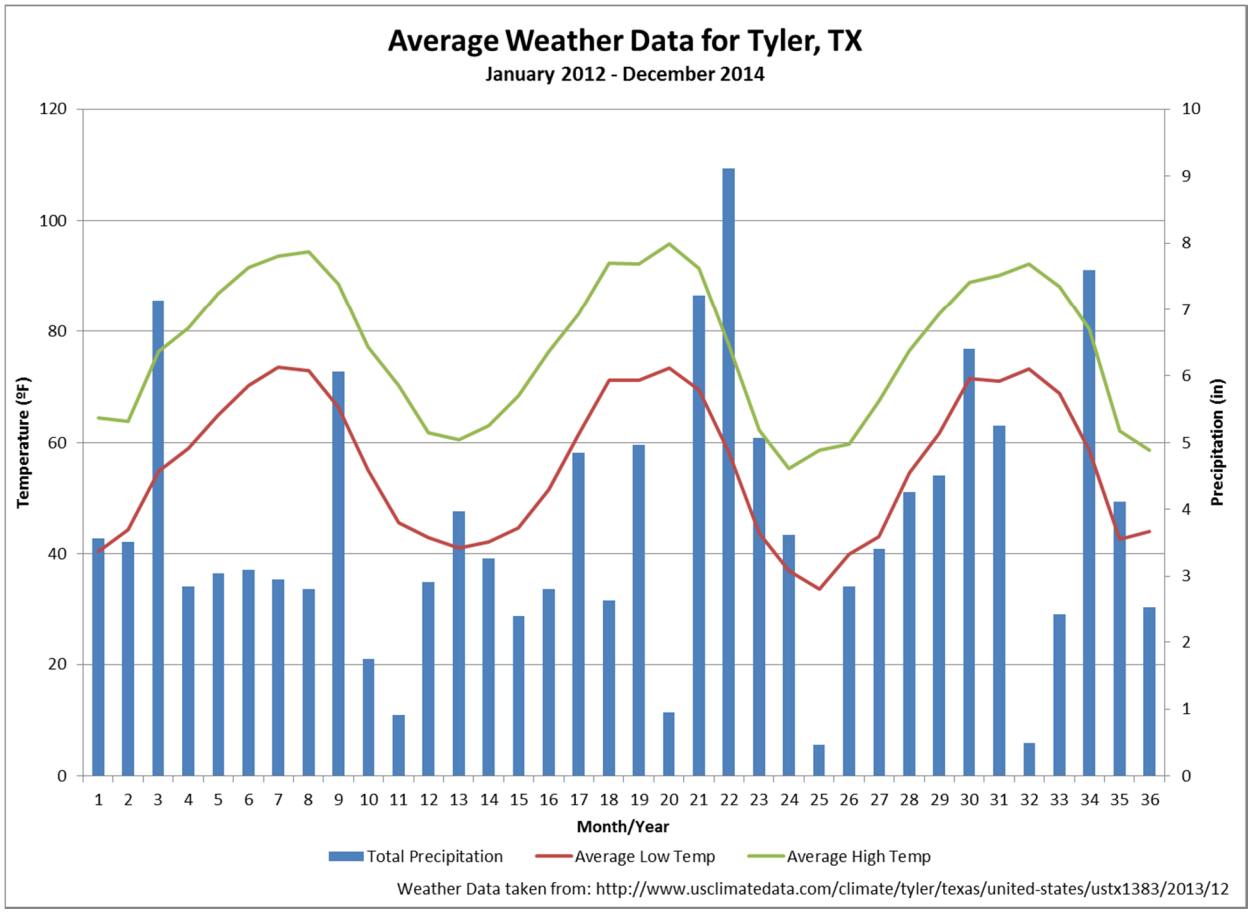

Figure 5. High and low temperature data as well as precipitation data for Tyler, TX as acquired by U.S. Climate Data.

This data would suggest that the PV performance will be higher during the May/June months and the lowest during November because of the lag between solar radiation cycles and temperature cycles as discussed in a later chapter.

3.2 Data Collected

3.2.1 Archival data

The archival data used for comparison in this study is the PV performance and weather data collected from TxAIRE House 2 during the middle of the third quarter of 2012 to the end of the fourth quarter of 2014.

Data collected for the house included the following pieces of information: total house energy, heat pump water heater energy, solar panel energy, roof temperatures, room temperatures, wall temperatures, CO_2 levels, and total solar radiation levels on the tilted surface. The variables of interest in terms of PV performance included: solar panel energy (W) and the total solar radiation on the tilted surface (W/m^2).

Weather data was also collected throughout the same time period mentioned previously. The weather data included the information given in Table 10, but is not limited to the information given in Table 10.

Table 10. Sample of weather data information collected.

Data Collected	Unit	Freqency of Collection
Average Temperature	°F	Average of 5 min period
High Temperature	°F	Average of 5 min period
Low Temperature	°F	Average of 5 min period
Average Humidity	%	Average of 5 min period
Wind Speed	mph	Instantaneous value
Wind Direction	NA	Instantaneous value
Pressure	in-hg	Instantaneous value
Rain Fall Amount	in	Total in 5 min period
Rain Fall Rate	in/hr	High in 5 min period
Solar Radiation	W/m^2	Average of 5 min period
Solar Energy	Langley	Total in 5 min period

Other collected information included data for the dew point, humidity, wind chill, heat index, and various other types of information such as the energy needed to heat and cool the building.

3.2.2 Purchased data from Meteonorm to create TMY and future TMY data sets

In order to perform a future performance prediction of the system, future typical meteorological year (TMY) data sets were needed. To obtain the future TMY, current TMY3 data sets were used with a method as described by Patton and further explained in this section. First, the TMY3 data set construction is explained. TMY3 data sets use data from the 1991 – 2005 National Solar Radiation Data Base (NSRDB) update. The TMY3 data set is made up of 12 typical meteorological months from January through December. These months are picked from different years over the period of record that is available. As an example, if the NSRDB has available 10 years of data for Tyler, Texas then all of the January data sets are examined and the month that is determined to be the most typical is included in the TMY3 data set for Tyler, Texas. All other months of the year would then be treated in the same manner and added to the TMY3 data set to create a complete year of data. Each month is selected based on using weighted statistics of the following characteristics: global horizontal radiation, direct normal radiation, dry-bulb temperature, dew-point temperature and wind speed. In the creation of the TMY3, the radiation characteristics are weighted the highest compared to the other three with the monthly mean and median and the persistence of weather patterns also taken into consideration.

The amount of data needed to construct a TMY was not available from the current archival data for TxAIRE House 2, therefore, it was decided that additional data needed to be purchased. Meteonorm is a comprehensive meteorological reference database with archival data from the Tyler/Pounds Fld Airport weather station (located approximately 11.6 miles west of the PV system location). Daily values for temperature, wind speed and dew point were purchased from the years 2004 – 2014. Daily radiation values were not available during this time frame, therefore TMY data sets for global, diffuse and beam radiation (calculated over a period of 19

years from 1991 – 2010) and temperature (calculated over a period of 9 years from 2000 – 2009) were also purchased.

With the TMY data set available, the projected change needed to be determined. The North American Regional Climate Change Assessment Program (NARCCAP) is an international program that produces high resolution climate change simulations in order to generate climate change scenarios [79]. NARCCAP uses global climate models combined with regional climate models to determine climate change from contemporary (1971 – 2000) to future (2041 – 2070) time periods. The data was extracted from the NARCCAP archive for the contemporary and future time periods for Tyler, Texas for temperature, wind speed and total global radiation. The TMY data for the contemporary time period was subtracted from the TMY data for the future time period; this resulted in the projected change data for each variable of temperature, wind speed and total global radiation. The projected change values were then added to the original TMY data set purchased from Meteonorm to create the future TMY data set.

3.2.3 How the data was collected and equipment used

The data for the house was collected using the NI-cRIO-9074 processor; a 400 MHz industrial real-time processor for control, data logging and analysis. PR-T24 thermocouple wires, polyvinyl insulated wires, were also used in retrieving the outside temperature. The data acquisition system (DAQ) was connected by USB to a personal software notebook to retrieve the data.

The weather data was collected from a Davis Vantage Pro 2 weather station situated above TxAIRE House 2 on the roof as shown in Figure 6. The weather station equipment collected data approximately every five minutes and the values taken were in various forms including: averages

over the five minute period, highs of the five minute period, lows of the five minute period, totals of the five minute period and instantaneous values taken at the time of data collection.

Figure 6. Location of weather station on roof of TxAIRE House 2.

Most of the data collected for weather and PV performance was taken every five minutes; however there were gaps in the data due to technical issues with the data logger equipment. To be able to use the data, the time and time intervals must be the same between the weather data and the PV performance data. To overcome the gaps in data, an interval of 30 minutes between readings was used for modeling in TRNSYS.

3.3 De Soto Modeling

The PV performance for this system was simulated using the TRNSYS simulation program. The simulation uses the one-diode, five parameter model to determine the overall performance of the system. Various five parameter models were discussed in high level detail in the previous chapter; however an in-depth look into De Soto's five parameter model will be reviewed to explain how the simulation model was calculating its values.

3.3.1 Current-voltage relationship for PV cells

The five parameter model can be expressed as shown in Figure 7 for an individual cell, for a module consisting of several cells, or for an array consisting of several modules as is the case for

the system in this study. The five parameter equivalent circuit consists of a current source (which represents the photocurrent that varies linearly with solar irradiation) in parallel with a single diode as well as a resistance in both parallel and series.

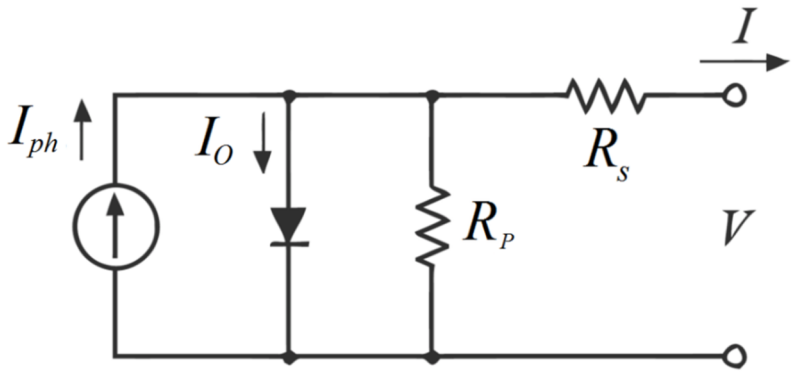

Figure 7. Five parameter equivalent circuit.

The equation derived from this model for the current-voltage relationship at a fixed cell temperature and solar radiation is expressed by Equations (14) and (15). The five parameter model is named as such because of the number of unknowns that must be determined in order to calculate the current and voltage and thus the power (the power is determined by multiplying the current by the voltage). The parameters/unknowns needed are: the photocurrent I_{ph}, the reverse saturation current of the diode I_O, the series resistance R_S, the parallel resistance R_P, and the modified diode ideality factor n.

$$I = I_{ph} - I_0\left[e^{\frac{V+IR_S}{n}} - 1\right] - \frac{V + IR_S}{R_P} \tag{14}$$

$$n \equiv \frac{N_S n_1 kT}{q} \tag{15}$$

The diode ideality factor n is a factor of the electron charge q, Boltzmann's constant k, the usual ideality factor n_1, the number of cells in series N_S, and the cell temperature T_C.

3.3.2 Calculating the five parameters

Three current-voltage pairs are normally available from the manufacturer at standard test conditions: the short circuit current (voltage is zero), the open circuit voltage (current is zero) and the current and voltage at the maximum power point (multiplication of both yields maximum power). The three current-voltage pairs are normally expressed by the typical I-V curve shown in Figure 8.

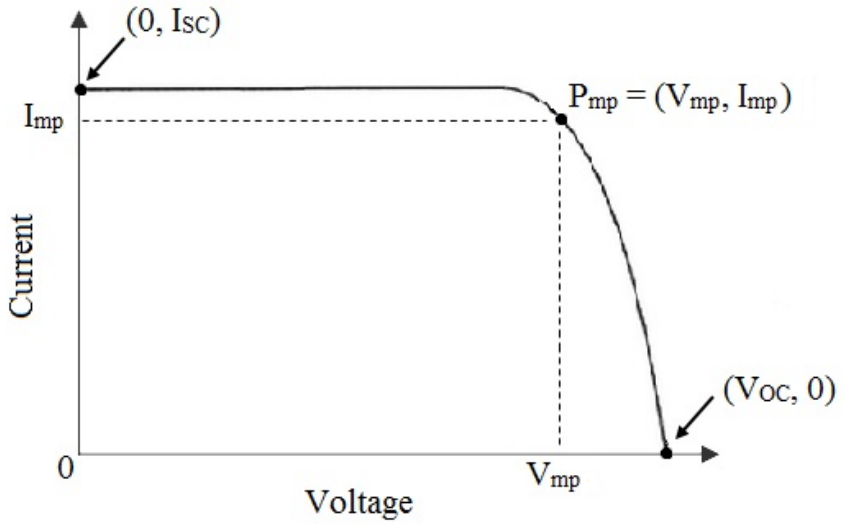

Figure 8. Typical I-V curve showing short circuit current, open circuit voltage and maximum power point.

To determine the values for the unknown parameters, these three known pairs at standard test conditions are substituted into Equation (14) resulting in Equations (56) – (59).

For short circuit current: $I = I_{SC}, V = 0$

$$I_{SC} = I_{ph} - I_O \left[e^{\frac{I_{SC} * R_S}{n}} - 1 \right] - \frac{I_{SC} * R_S}{R_P} \tag{56}$$

For open circuit voltage: $I = 0, V = V_{OC}$

$$0 = I_{ph} - I_O \left[e^{\frac{V_{OC}}{n}} - 1 \right] - \frac{V_{OC}}{R_P} \tag{57}$$

At maximum power point: $I = I_{mp}, V = V_{mp}$

$$I_{mp} = I_{ph} - I_O \left[e^{\frac{V_{mp}+I_{mp}*R_S}{n}} - 1 \right] - \frac{V_{mp} + I_{mp} * R_S}{R_P} \quad (58)$$

The derivative with respect to power at the maximum power point is zero.

$$0 = I_{mp} - V_{mp} \left[\frac{\frac{-I_O}{n} * e^{\frac{V_{mp}+I_{mp}*R_S}{n}} - \frac{1}{R_P}}{1 + \frac{I_O * R_S}{n} * e^{\frac{V_{mp}+I_{mp}*R_S}{n}} + \frac{R_S}{R_P}} \right] \quad (59)$$

This left five equations, (Equations 15, and 56 – 59), and five unknowns (I_{ph}, I_O, R_S, R_P, and n) as V_{OC}, I_{SC}, I_{mp} and V_{mp} were given by the manufacturer. The equations were then solved simultaneously for the conditions given by the weather data. With the five unknowns calculated, the current could then be calculated at specific voltage points using Equation 14; the results from this gave the data points for the I-V curve. The current and voltage were then multiplied to get the predicted max power at specific voltage points. The next section covers the simulation used in TRNSYS to determine the power output incorporating the weather data and an inverter.

3.4 TRNSYS Modeling

3.4.1 Overall system

TRNSYS was the software package used to simulate the PV system. This software package uses the one-diode, five parameter model as explained in the previous section. The simulation had the basic outline as shown in Figure 9 which uses the following components: Type9 (user entered data labeled as Weather Data), Unit Conversion (to convert units to SI), Type 194b PV-Inverter (uses five parameter model as presented by De Soto to solve labeled as PV-Inverter) and Type65d (graphs the output data labeled as Graph Output). The component labeled “Start and Stop Times” was the area in which to input the start and stop time of the simulation. Weather data was input into the Type9 component as a CSV file with temperature, total radiation on the tilted surface and wind speed along with the date and time. These values were then converted

into SI units with the unit conversion component and input into the Type 194b PV-Inverter component and output graphically using Type65d. The components labeled Radiation and Power Output, Voltage, Current also output those data points for the simulation as a .dat file that could then be opened with excel.

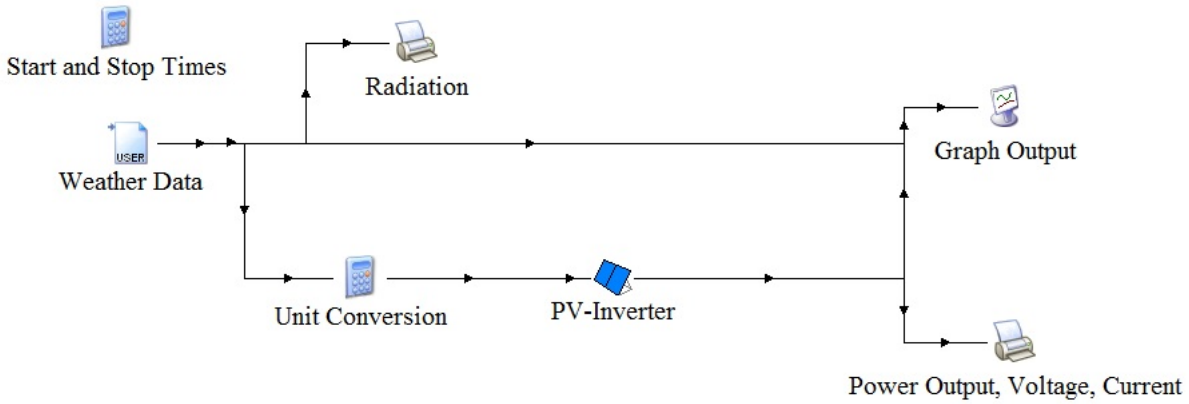

Figure 9. TRNSYS simulation setup.

3.4.2 Component overview

The first component in the system is the controls (labeled as Start and Stop Times). The start time and stop time are input into this component in terms of hours of the year. For example, if the data file starts on the 145th day of the year at midnight, then the input for start time would be 3480 (24 * 145).

One of the most important components in the simulation is the Type9 component (labeled Weather Data). Type9 is a component that reads data at regular time intervals from a user defined data file. This allows for the user to input data from weather data recorded experimentally rather than taken from the weather database that is included in the TRNSYS package. The weather data recorded from 2012-2014 was formatted to be accepted by the Type9 component. This formatting is discussed in a later chapter. The component then read the data for the solar radiation, temperature and wind speed and output it to the unit converter in terms of

W/m^2, Fahrenheit and mph, respectively. Figure 10 shows the data that is output from the Type9 component.

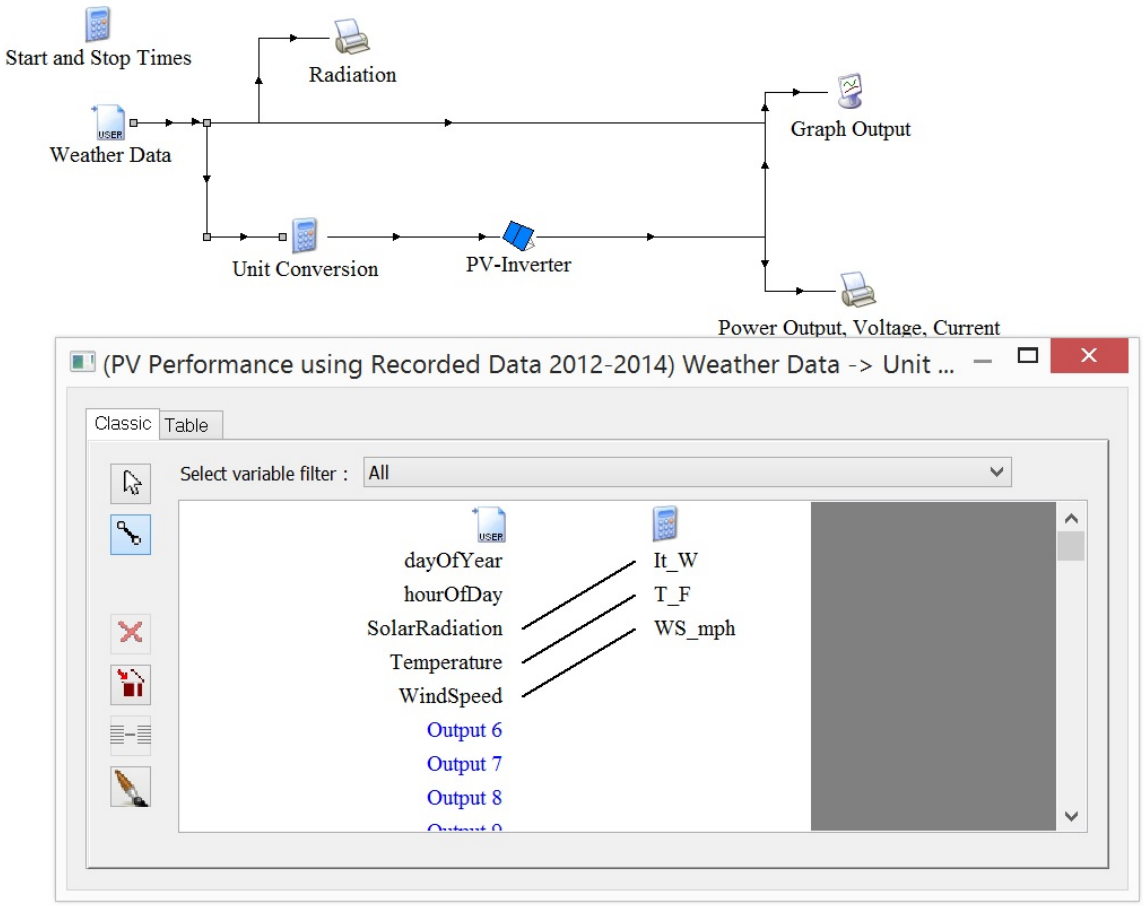

Figure 10. Solar radiation, temperature, and wind speed output from Type9 component to be input to the Unit Conversion component.

The Unit Conversion component then converted the units to SI units to be input into the Type194b PV-Inverter component.

The most important component in the simulation was the Type194b PV-Inverter component. Type194b determines the electrical performance of a photovoltaic array and may be used with simulations involving electrical storage batteries, direct load coupling or utility grid connections such as the system used in this study. The model determines the current and power of the array at a specified voltage and will also output the current and voltage at the maximum power point.

This component uses De Soto's one-diode, five-parameter model to calculate the PV performance. There are other models in TRNSYS to determine the output of PV systems; however this component differs from the others in that it also considers the effects of the inverter and its efficiency. Therefore, this component was chosen to model the PV system because of the added calculation of the inverter efficiency. The inputs of the component come from two sources. One source is the outputs of the Type9 weather data file which are the solar radiation, temperature and wind speed. The other source is from user input of the solar panel parameters mentioned in the previous chapter. Figure 11 shows the input from the Unit Conversion component.

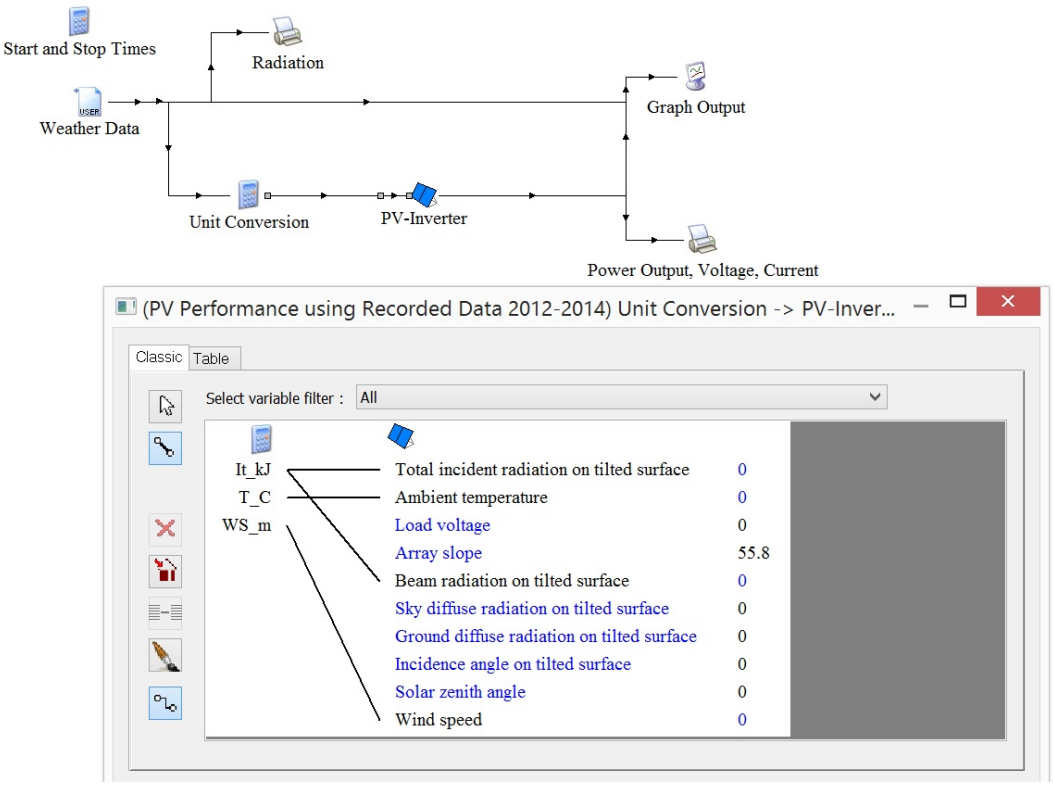

Figure 11. Solar radiation, temperature, and wind speed in SI units output from the Unit Conversion component to be input to the Type194b component.

The radiation had been converted to kJ/m^2, the temperature to Celsius and the wind speed to m/s.

The last part of the simulation file output the data from Type194b into a graph using component Type65d. Figure 12 shows the original output from the weather data being input to the graphing component along with PVPower which is the output from Type194b of the PV performance.

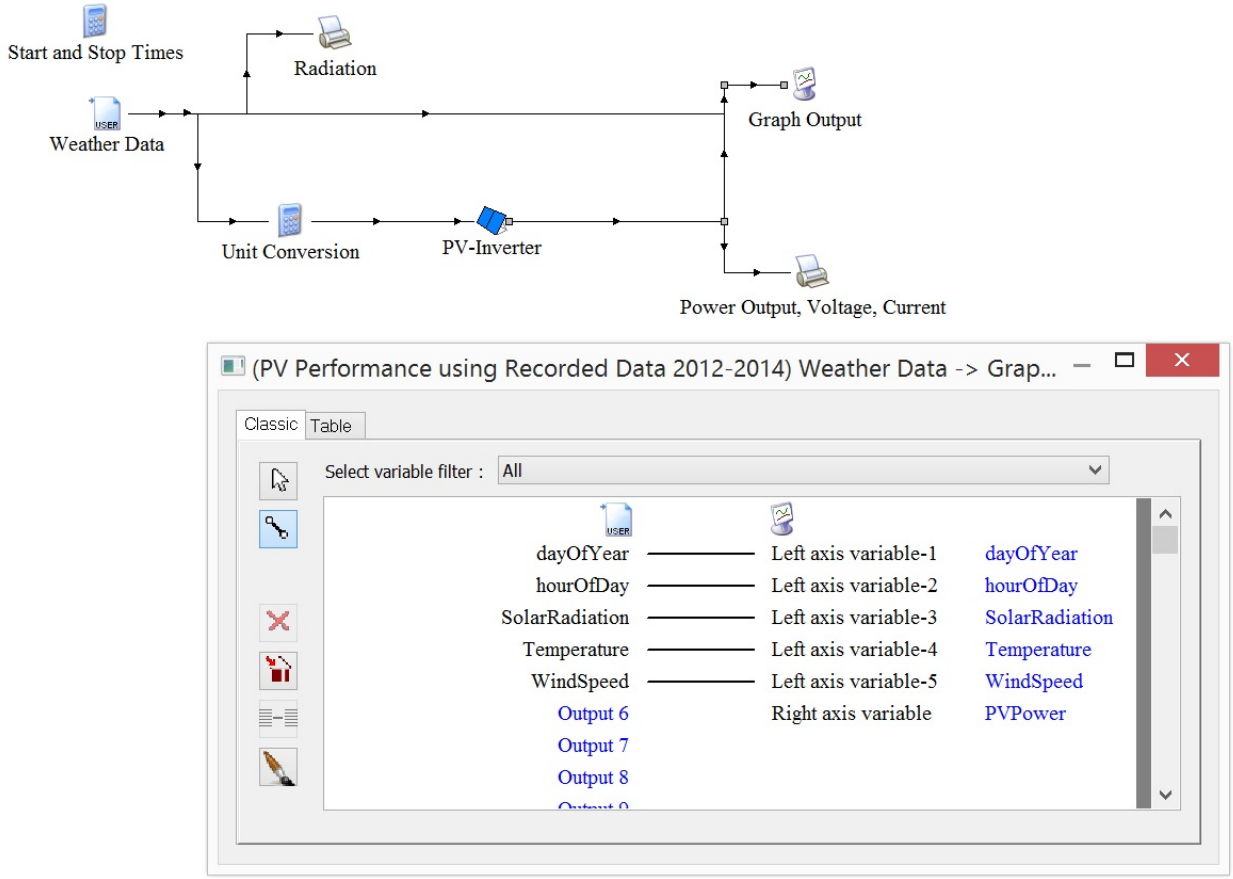

Figure 12. Solar radiation, temperature, wind speed, and date and time output from the Type194b component to be input to the Type65d component for graphical output.

Type65d is an online graphics component used to display selected variables while the simulation is progressing. The component was used to display solar radiation, temperature, wind speed and PV power against date and time. The power at maximum power point, open circuit voltage and the short circuit voltage were also output into an external data file as shown in Figure 13.

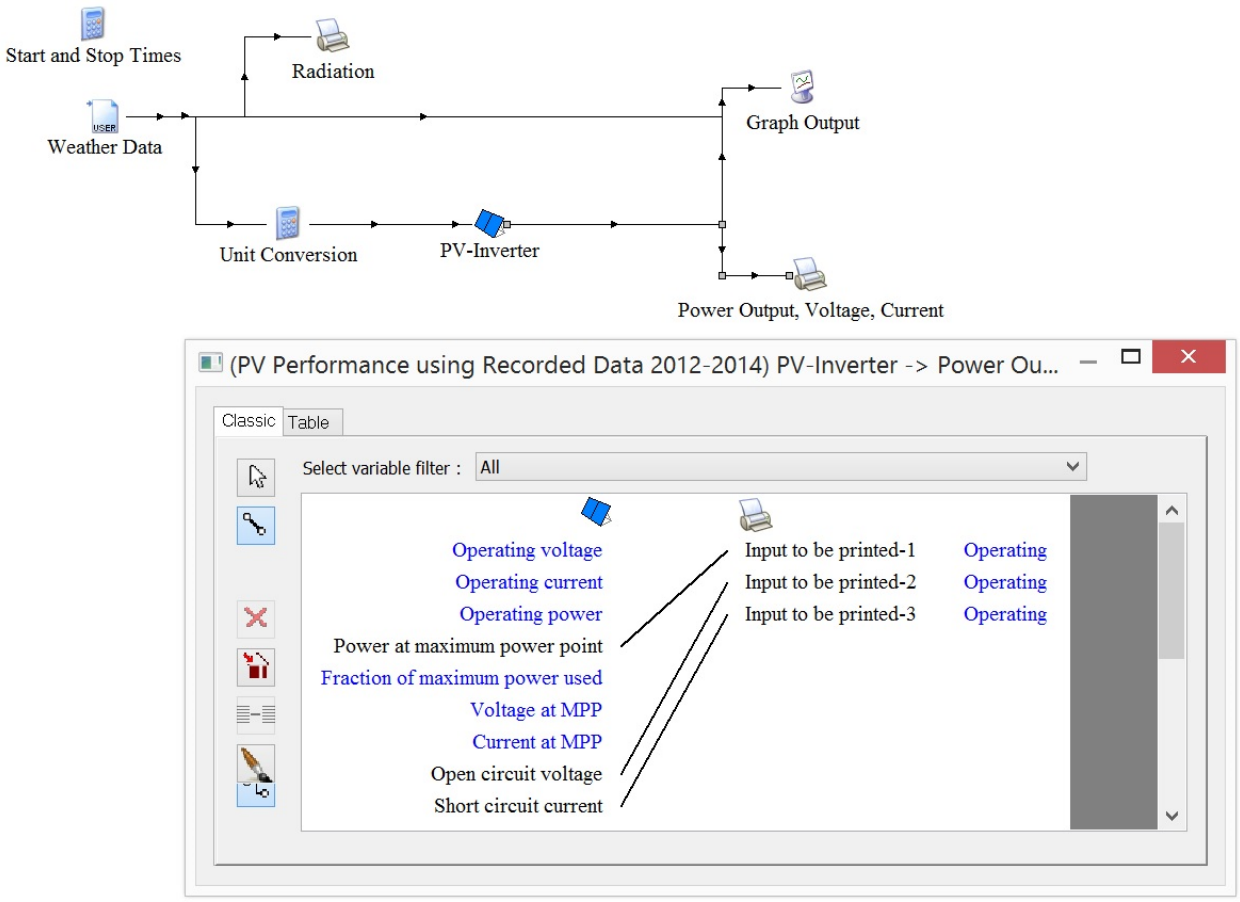

Figure 13. Output from Type194b of power at maximum power point, open circuit voltage and short circuit current to external data file.

3.5 Summary and Conclusions

After the data was collected and formatted for the three year period between 2012 and 2014, the simulation for the PV panels used by TxAIRE House 2 was ran using the TRNSYS software with collected experimental data to show predicted performance. The I-V curve for the modules used in the PV system was created using De-Soto's five-parameter model to also show predicted performance. In order to determine future performances, weather data over several years was collected and formatted to create what is known as the typical meteorological year which was created by reviewing long-term climate records and linking months together from selected years to represent long-term conditions of solar radiation and average temperature. The simulation was

then run again using the typical meteorological year to determine long-term system performance. Data was also extracted from the typical meteorological year to provide future typical meteorological years for future performance predictions using the TRNSYS model discussed.

Chapter 4

Experimental Results and Model Validation

The results of the predicted PV output for TxAIRE House 2 using recorded and purchased weather data with the TRNSYS simulation software, as well as the results for future performance as predicted with the future typical meteorological year are presented in the following sections.

4.1 Performance Using Five-Parameter Model

The TRNSYS software package included a plugin with the Engineering Equation Solver (EES) software. EES is a general equation-solving program that can numerically solve thousands of coupled non-linear equations, such as that of the five-parameter model proposed by De Soto. The equation solver required the following parameters: number of cells in series with each module, open circuit voltage, short circuit current, max power voltage, max power current, the temperature coefficient of short circuit current and the temperature of open circuit voltage. All of the information was included in the manufacturer data sheet for the modules used in the PV system in this study.

The EES program then solved the non-linear Equations 15, and 56 – 59 discussed previously to determine the five unknown parameters. Figure 14 shows the inputs and outputs using EES. The variables output from the program are: n, the usual ideality factor (labeled a_{ref}); I_{PH}, the photocurrent (labeled $I_{L,ref}$); I_O, the reverse saturation current of the diode (labeled $I_{O,ref}$); R_S, the series resistance and R_P, the resistance in parallel (labeled $R_{SH,ref}$).

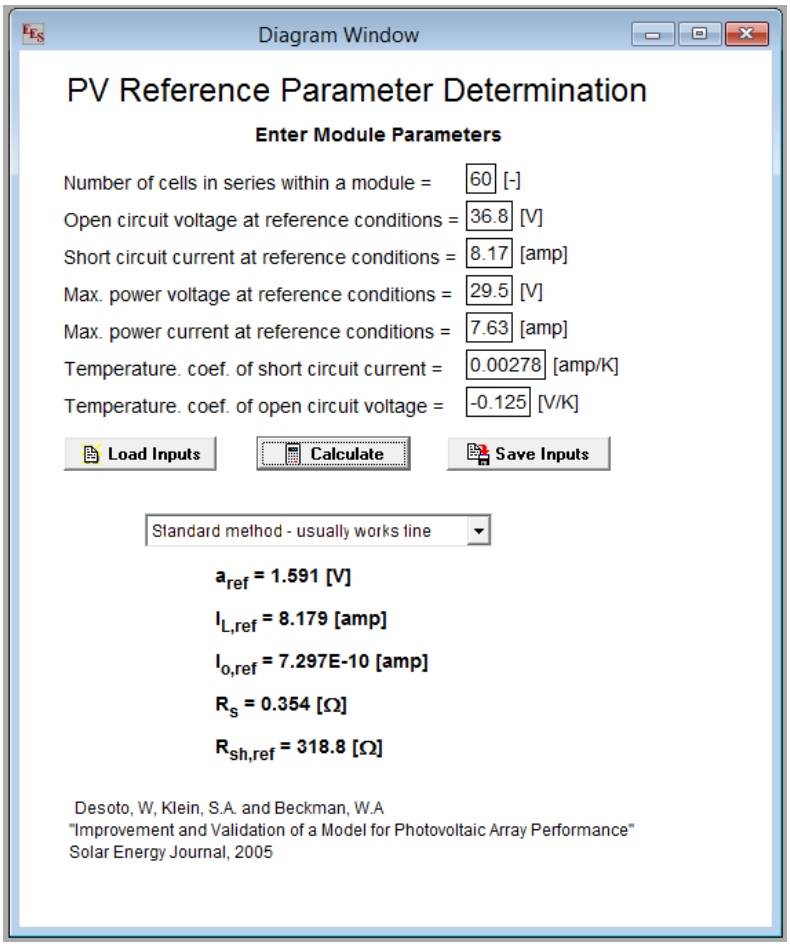

Figure 14. Input and output of the EES program for De Soto's five-parameter model.

Using the calculated parameters, the current at specified voltage points was calculated using Equation 14 in Microsoft Excel.

$$I = I_{ph} - I_0\left[e^{\frac{V+IR_S}{n}} - 1\right] - \frac{V + IR_S}{R_P} \tag{14}$$

Figure 15 shows how Equation 14 was input into Excel using the calculated parameters to calculate current. The current was calculated with the parameters for values of voltage from zero to the open circuit voltage value of 36.8 V.

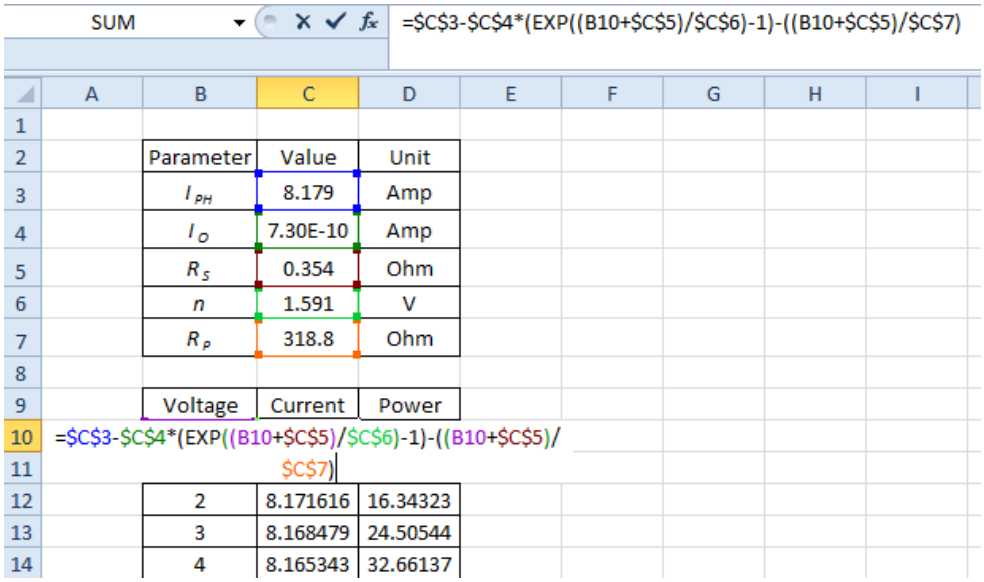

Figure 15. Example of Equation 14 as written in Excel with input parameters.

The power was calculated by multiplying the calculated current and the voltage as shown in Figure 16.

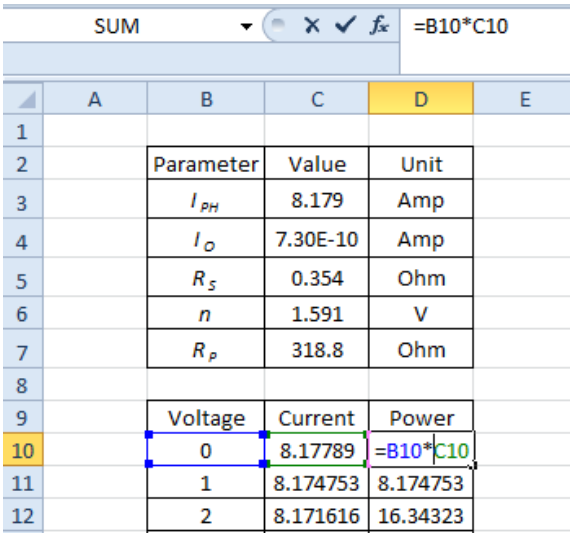

Figure 16. Example of power calculation by multiplying voltage and calculated current in Excel.

This information was then used to graph the current along with power in terms of voltage to create both the I-V and P-V curves. Figure 17 shows the I-V and P-V curves for the modules used in the PV system for this study.

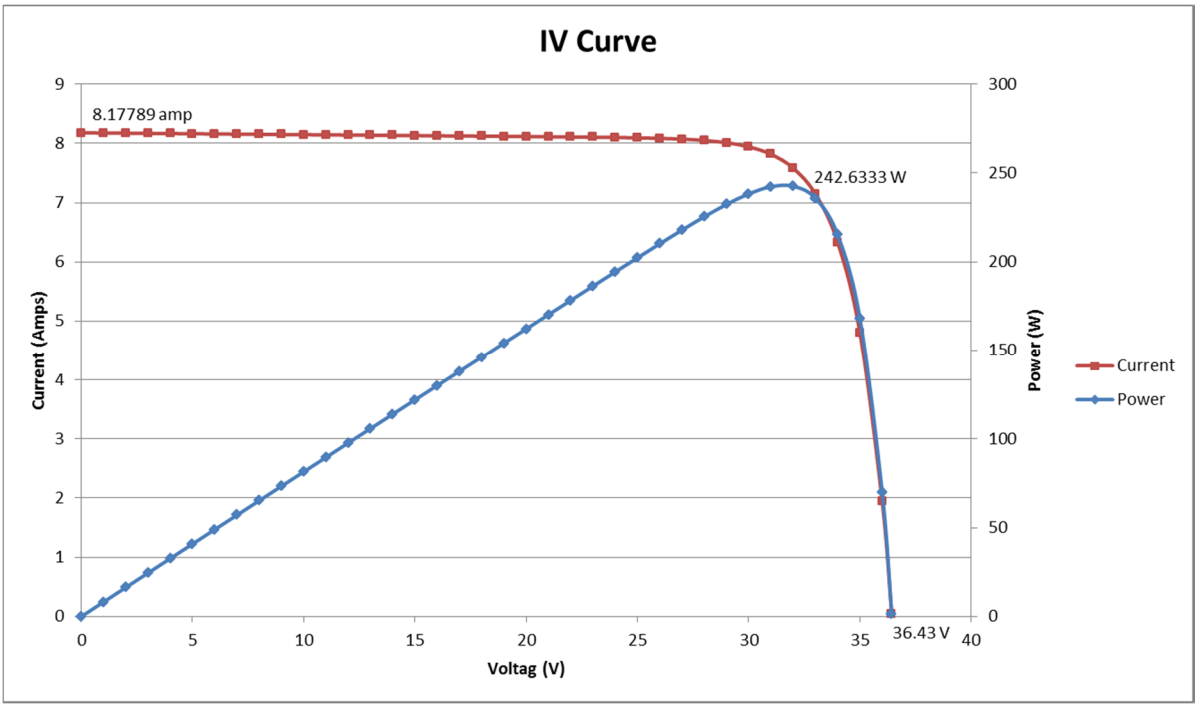

Figure 17. I-V and P-V curves for Sunmodule modules calculated using De Soto's five-parameter model.

The calculated I-V and P-V curves match the information provided by the manufacturer in that the highest calculated current was 8.17789 amps (8.17 amps on the data sheet), the highest voltage calculated before giving negative current values was 36.43 V (36.8 V on the data sheet) and the highest predicted power was calculated to be 242.6333 W (225 W on the data sheet).

Since there are 33 modules in the system, De Soto's model predicted a max power output of 8006.89 W (power output per module multiplied by number of modules). De Soto's five-parameter model predicts the maximum performance of the system without taking into account the actual weather data, inverter or losses in the system. The next section will review the TRNSYS simulation results which take into account these factors.

4.2 PV Performance Using Recorded Weather Data

4.2.1 Experimental recorded weather data

The data recorded from TxAIRE House 2 came from the NI-cRIO-9074 data logging processor, PR-T24 thermocouple wires and a Davis Vantage Pro 2 weather station situated above the house. The data of interest to this simulation included the: total incident radiation on the tilted surface (recorded with the NI-cRIO-9074 data logging processor), outside temperature (recorded using the PR-T24 thermocouple wires) and wind speed (recorded using the Davis Vantage Pro 2 weather station). The date and time were also recorded for all variables. These variables were recorded using several pieces of equipment and therefore had been recorded in different time intervals. To use the data, the time intervals had to be consistent between the variables needed in the simulation. The smallest time interval consistent between the variables was 30 minutes, therefore the data was modified to only include the instantaneous values at 30 minute intervals for all of the variables mentioned. The data also included bad readings which resulted in negative values for radiation which is not possible. Therefore all negative values for radiation were removed from the data set. Table 11 shows an example of the modified data set. The data shown in Table 11 was used in the TRNSYS simulation to determine the PV performance between the middle of the third quarter of 2012 to the end of the fourth quarter of 2014. The first column is the day of the year followed by the second column which shows the time of the day in decimal format. Radiation in $\frac{W}{m^2}$, temperature in ºF and wind speed in mph make up columns 3 – 5.

Table 11. Example of modified data set.

Date (Day of the Year)	Time (Time of the Day)	Incident Radiation on Tilted Surface (W/m^2)	Temp Out (°F)	Wind Speed (mph)
213	7	9.105	77	4
213	7.5	23.0946	77.3	5
213	8	62.106	78.1	5
213	8.5	174.618	79.4	6
213	9	298.548	80.5	5
213	9.5	410.268	82.1	7
213	10	508.2	83.8	5
213	10.5	605.52	86.4	4
213	11	687.72	87.7	4
213	11.5	767.7	89.1	5
213	12	825.6	90.8	6
213	12.5	873.12	92.7	7

Figure 18 shows the relationship between the total incident radiation on the tilted surface and the outside temperature over the analysis period. During the winter months there was an average decrease in temperature of 76ºF between the highest temperature of the summer months and the lowest of the winter months. During the winter months, as temperatures were decreasing, there was a slight increase of an average of 36 $\frac{W}{m^2}$ in recorded radiation. Figure 18 shows the spikes in temperature between the months of June – September with temperatures reaching above 90ºF for an average of 14 days in a row during these months. The radiation values peaked daily during the hours of 10:00 AM and 5:00 PM ± 1 hour, with overall decreasing values during the summer months of 36 $\frac{W}{m^2}$ as mentioned above.

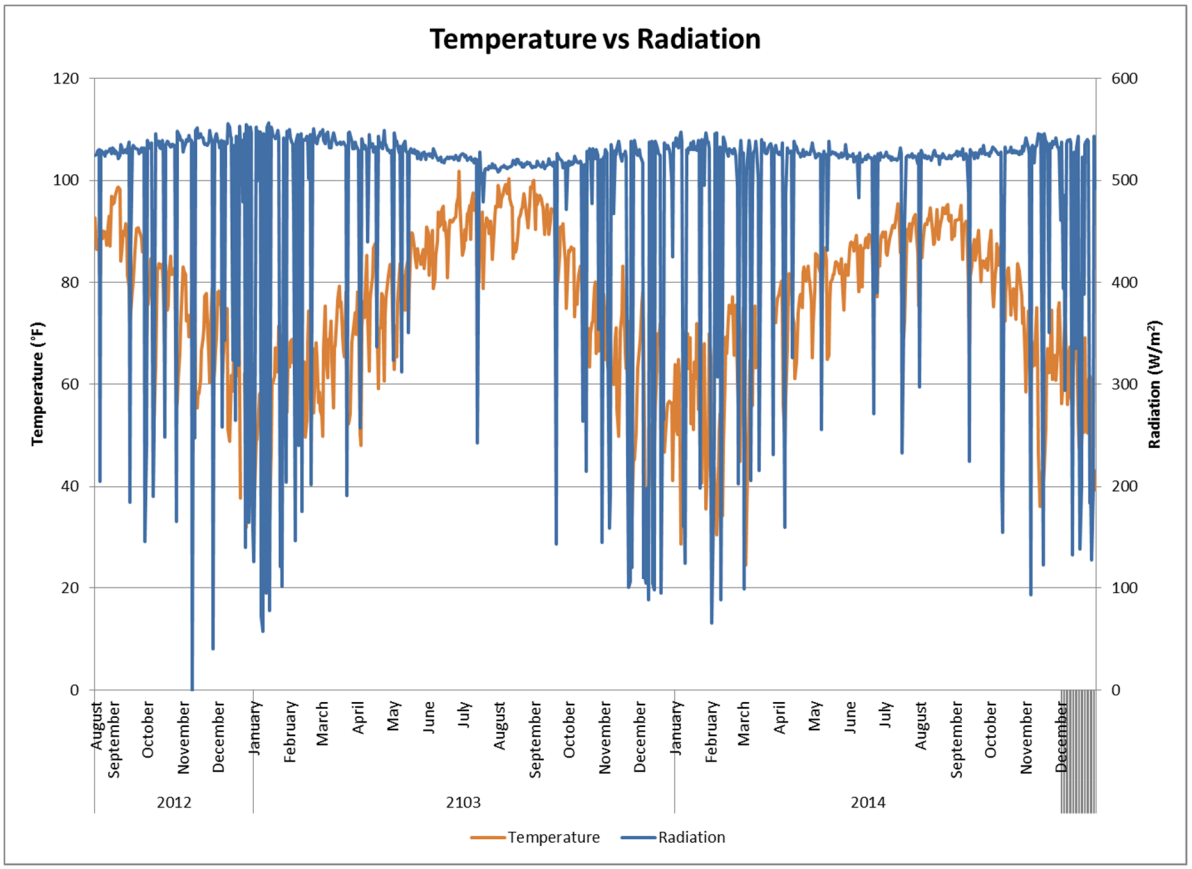

Figure 18. Overall recorded data of temperature and radiation over time.

Figure 19 shows the trend for wind speed over the analysis time period. This chart shows the highest wind speed for each day for the time period. During the winter months, the overall wind speed was generally higher than in the summer months with approximately 7 mph difference between summer and winter.

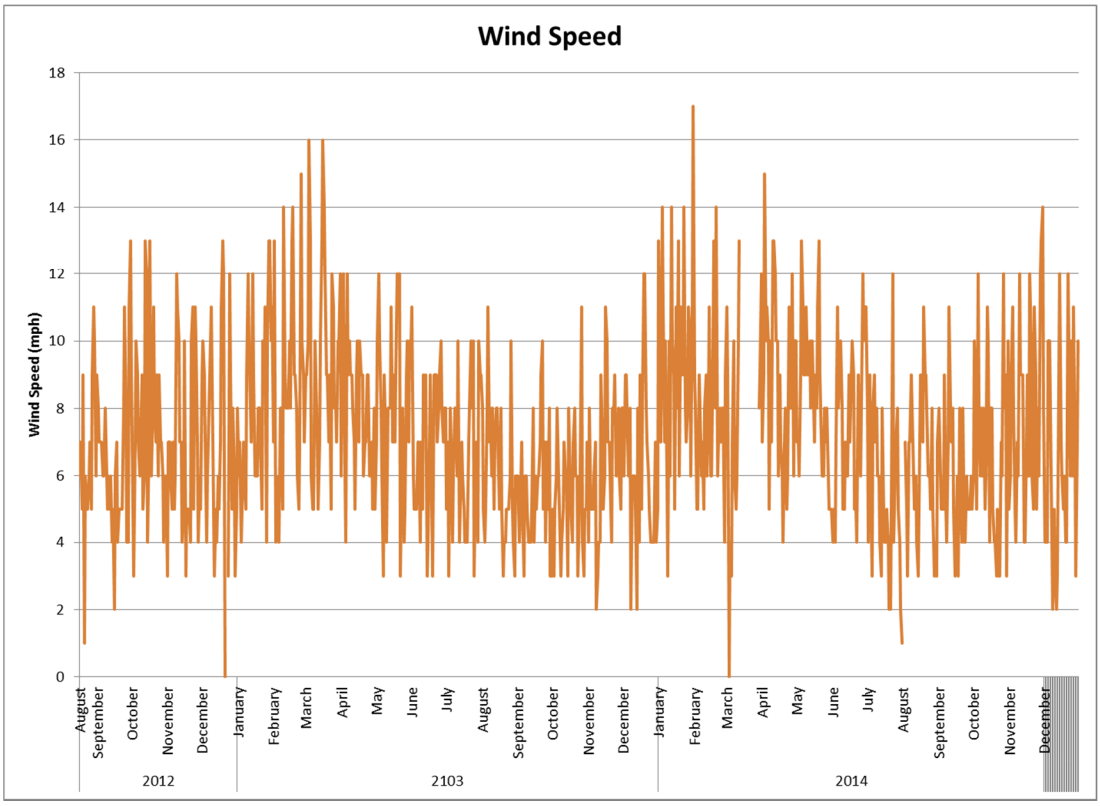

Figure 19. Overall recorded data of wind speed over time.

4.2.2 TRNSYS Simulation Results

The PV performance was determined using the methods described in the previous chapter with the TRNSYS software using first the recorded data as detailed previously. The graphical output of the TRNSYS software is shown in Figure 20 as a comparison of all the variables (date/time, total incident radiation, temperature and wind speed) with the predicted PV output as determined using the five-parameter model in the software package.

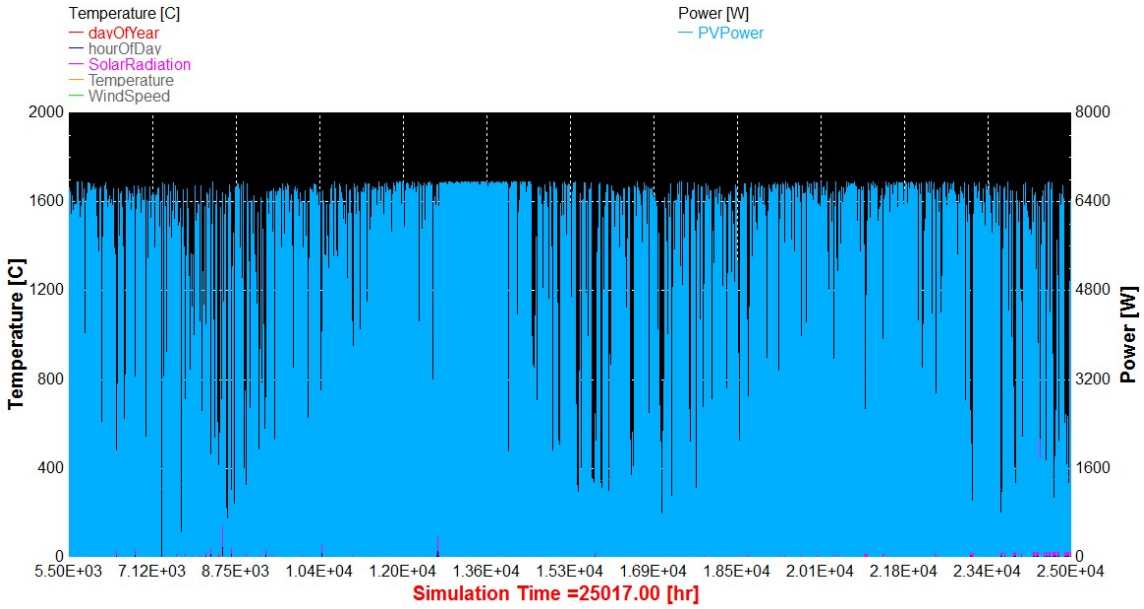

Figure 20. TRNSYS output results of solar radiation and power over time.

As shown, the power output has a maximum output of 6770.99 W. The TRNSYS simulation had a max power output of 6770.99 W showing 91% efficiency from the manufacturer max power of 7425 W. To determine the accuracy of the simulation, the power output was compared to the power output as recorded by the NI-cRIO-9074 data logging processor for the years used in this study. Figure 21 shows the correlation between the predicted PV output and the recorded output as a function of radiation.

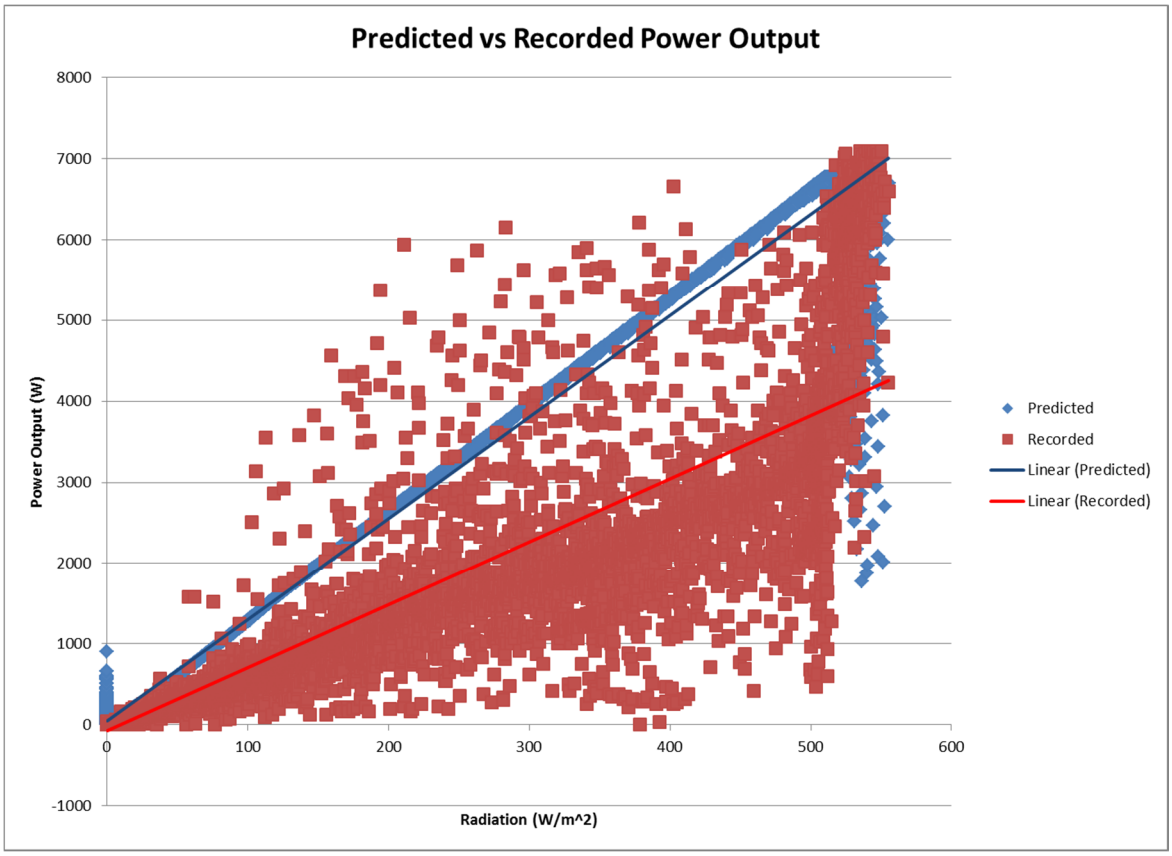

Figure 21. Predicted versus recorded power output in terms of radiation.

The average value for recorded power was calculated to be 783 W with a max of 7095 W. The average value for predicted power was calculated to be 1431 W with a max of 6771 W. The percent difference between both the averages was -45% and maximums was -5%.

4.3 Meteonorm Purchased Data Validation

Using the recorded data to predict the PV performance was the most accurate weather data that could be used for the simulation as it was recorded at the site of the solar panels, however, the overall time the data was recorded (2012 – 2014) was not sufficient to create a typical meteorological year and future typical meteorological year for predicted future performance as discussed in the previous chapter. To obtain this, weather data was purchased from Meteonorm for the years of 2004 – 2014 for the global, diffuse and beam radiation, outside temperature and

wind speed recorded from the Tyler/Pounds FLD weather station. This data was then compared to the recorded data to determine accuracy as shown in the following sections.

4.3.1 Purchased weather data

The weather data from Meteonorm included daily values for outside temperature, wind speed and dew point as mentioned in the previous chapter. The daily values were not recorded during the time period for global radiation; therefore the TMY data (created from a data set between 1991 – 2010) for global, diffuse and beam radiation was supplied.

Figure 22 and Figure 23 show the data between the recorded and purchased outside temperature and wind speed for the years 2012 – 2014, respectively. The average monthly values of the purchased data were compared to average monthly values obtained from the recorded data.

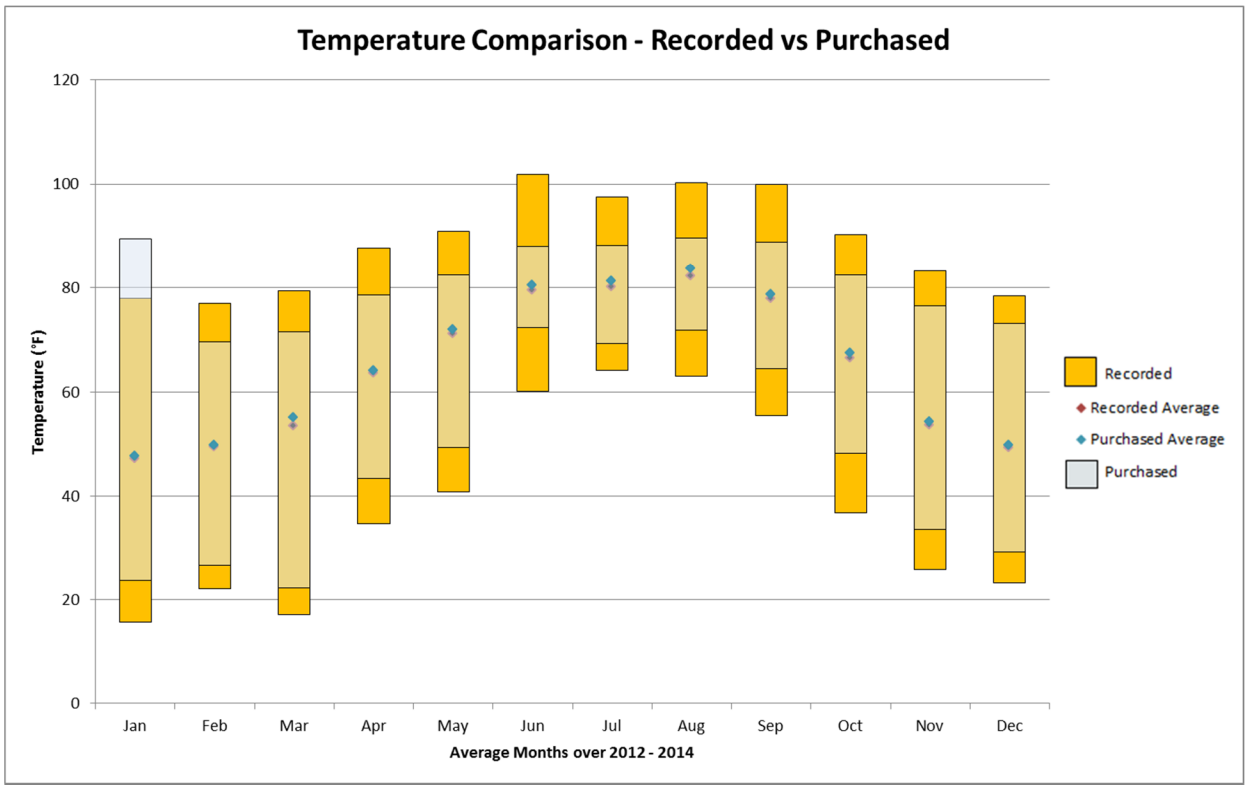

Figure 22. Temperature comparison of recorded and purchased data using minimum, average and maximum data points.

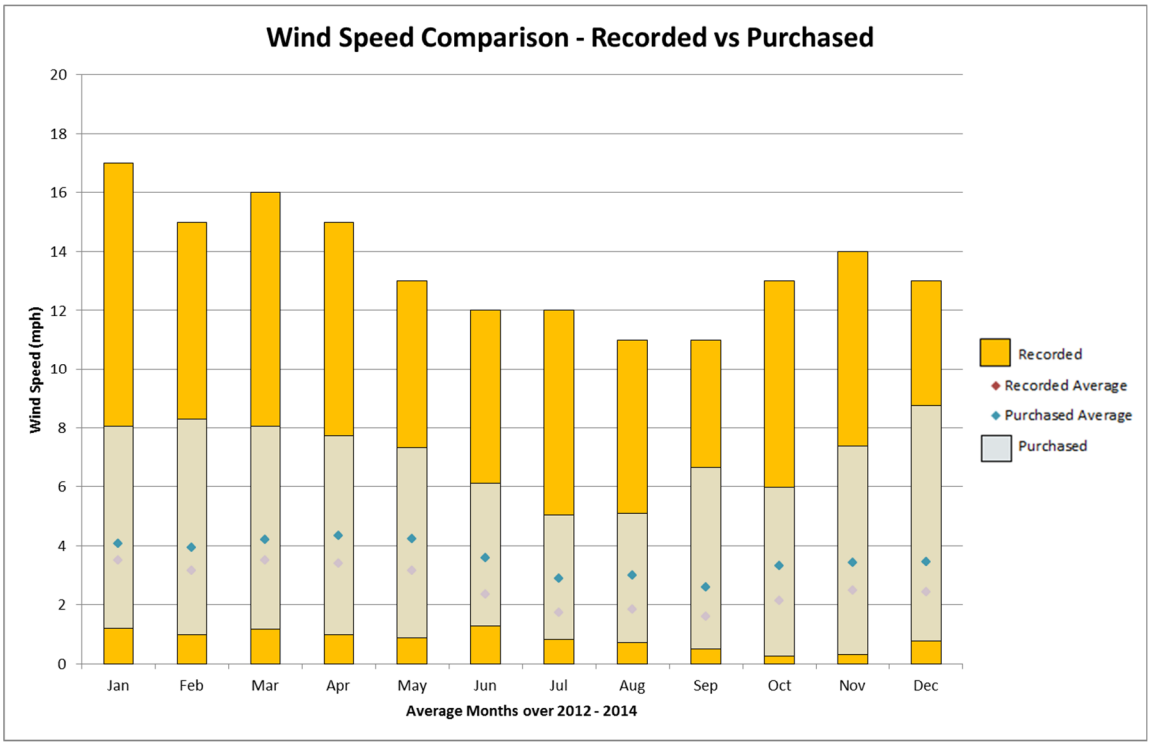

Figure 23. Wind Speed comparison of recorded and purchased data using minimum, average and maximum data points.

In general, both the temperature and wind speed comparisons followed the same trend; however the data showed that the purchased data did not capture the more extreme weather conditions that were seen by the weather station at TxAIRE House 2. The averages for each month for the temperature comparisons had an average percent difference of 1.31%. The averages for each month for the wind speed comparisons had a much higher average percent difference of 41.53%.

Figure 24 shows the data between the recorded and purchased radiation values for the years 2012 – 2014. Monthly averages of the total incident radiation on the tilted surface obtained from the recorded data were compared to the total radiation values provided by Meteonorm.

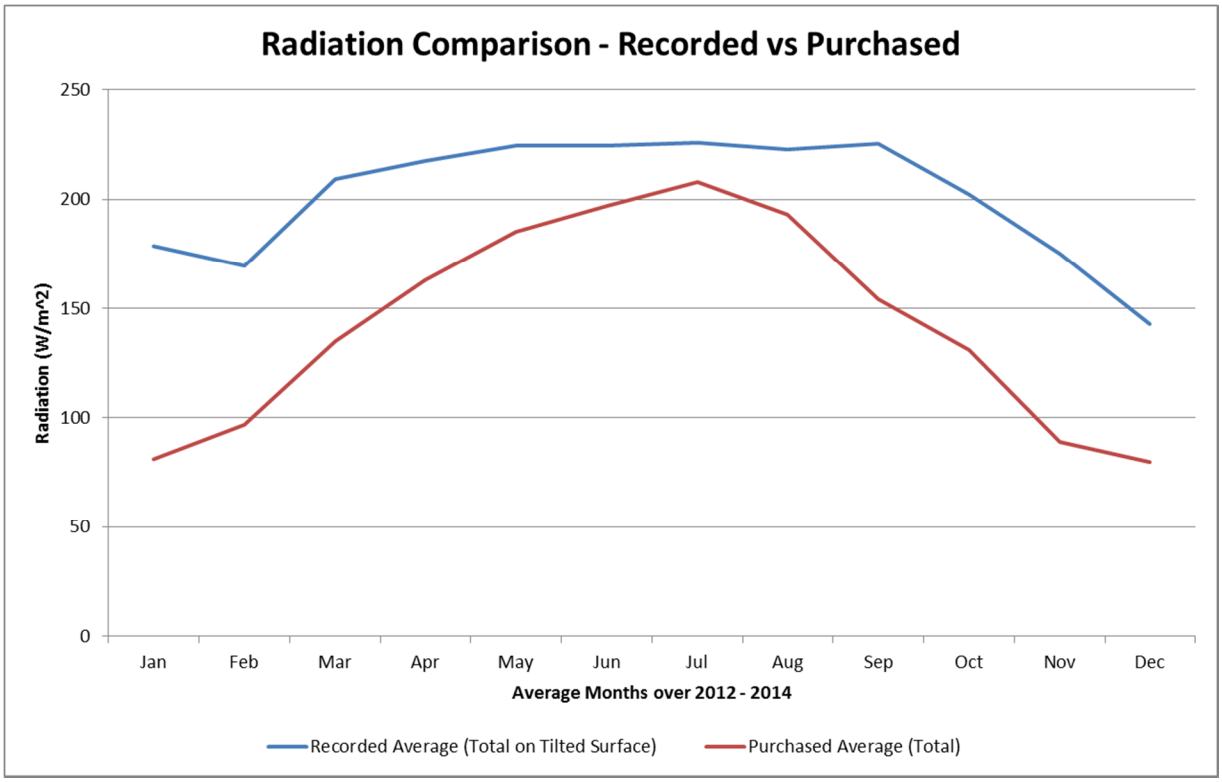

Figure 24. Radiation comparison of recorded and purchased data using average and TMY data points.

The radiation comparison also shows the same general trend between the purchased data and the recorded data. However, the difference in percentage averages shows a 30.76% decrease of the purchased data vs the recorded data.

4.4 PV Performance using the Typical Meteorological Year

According to the research, it is customary to use a typical meteorological year to run long-term system performance simulations [75]. The creation of the TMY data set was described previously by combining statistically the most typical data of each month from several years of archival data together to create a typical meteorological year. Meteonorm supplied daily values for the temperature and wind speed over a 10 year period between 2004 – 2014, as well as TMY data for temperature (over a period of 9 years from 2000 – 2009) and radiation (over a period of 19 years from 1991 – 2010). The wind speed data purchased from Meteonorm was used to create

the typical meteorological year data over a 10 year period between 2004 – 2014 to add to the given typical meteorological year data set.

4.4.1 Future typical meteorological year

The predicted performance simulation for the years 2012 – 2014 using the recorded data used total incident radiation on the tilted surface, outside temperature and wind speed to determine the performance. To be consistent, the TMY needed to also have the same variables as used in the previous simulation. The purchased data from Meteonorm included the TMY data for temperature and total radiation, therefore the typical meteorological year data for wind speed needed to be calculated.

To calculate the TMY data for wind speed over 10 years, the average wind speed of each day for each month was reviewed against the same month for every year of data purchased. The mean was calculated and the month with the closest data point to the mean was picked to be included in the TMY data set. The average value for the following months were used to create the TMY for wind speed: January 2004, February 2004, March 2011, April 2008, May 2007, June 2009, July 2012, August 2014, September 2009, October 2013, November 2004, and December 2010. With the TMY data for wind speed created, the full TMY data set was created as shown in Table 12.

Table 12. TMY data set for Tyler, Texas using Meteonorm data.

Month	Temperature	Radiation	Wind Speed
	(°F)	(W/m^2)	(mph)
Jan	47.84	81	3.93
Feb	51.08	97	4.09
Mar	58.64	135	4.50
Apr	65.84	163	4.72
May	73.22	185	3.18
Jun	79.16	197	3.39
Jul	82.58	208	2.98
Aug	82.94	193	2.99
Sep	76.46	154	2.51
Oct	66.74	131	3.05
Nov	57.2	89	3.65
Dec	48.02	80	4.26

This data was then used to create a future TMY data set using the method described in the previous chapter. The projected climate change in terms of values for temperature, radiation and wind speed were extracted from the NARCCAP database. NARCCAP uses global and regional climate models to predict climate change from contemporary (1971 – 2000) to future (2041 – 2070) time periods. The value of change between the future and contemporary values were calculated and are shown in Table 13. NARCCAP predicts an average temperature increase of 36.11ºF, an average radiation increase of 11.67 $\frac{W}{m^2}$ and an average decrease of wind speed of -.12 mph.

Table 13. Predicted change values for Tyler, Texas using NACCARP predicated values.

Month	Temperature Change	Radiation Change	Wind Speed Change
	(°F)	(W/m^2)	(mph)
Jan	35.06	12	-0.18
Feb	34.88	9	-0.04
Mar	34.7	14	-0.02
Apr	35.24	7	-0.29
May	36.32	13	-0.07
Jun	37.22	13	-0.09
Jul	37.58	8	0.07
Aug	37.22	14	-0.02
Sep	36.5	13	-0.22
Oct	36.32	12	-0.25
Nov	35.96	8	-0.11
Dec	36.32	11	-0.18

The projected change values were added to the original TMY data to give the future typical meteorological year. The future TMY predicts typical values from predicted values for the years 2041 – 2070. The future TMY data set is shown in Table 14.

Table 14. Future TMY data set for Tyler, Texas using Meteonorm data plus the predicted change value from NARCCAP data.

Month	Temperature	Radiation	Wind Speed
	(°F)	(W/m^2)	(mph)
Jan	82.9	93	3.75
Feb	86.14	106	3.92
Mar	93.7	149	4.32
Apr	100.9	170	4.54
May	108.28	198	3.00
Jun	114.22	210	3.21
Jul	117.64	216	2.80
Aug	118	207	2.81
Sep	111.52	167	2.33
Oct	101.8	143	2.87
Nov	92.26	97	3.47
Dec	83.08	91	4.09

4.4.2 TRNSYS simulation results for future predicted performance

The PV long-term performance was determined using the methods mentioned in the previous section with the TRNSYS software, using the TMY and future TMY data sets shown Table 12 and Table 14, respectively. Figure 25 shows the results of the power output based on Meteonorm TMY and the future TMY created using the original Meteonorm TMY and predicted change data by NARCCAP.

The biggest contributing factor to the power output between temperature, radiation and wind speed was radiation. Comparisons between the purchased radiation and the recorded radiation showed a percent decrease of 31% from the recorded to the purchased as seen in a previous section. This difference shows up in the power output using the TMY data sets. The power output for the current Meteonorm TMY data set showed a max power output of 2747.41 W during the month of June as seen in Figure 25. Using the future TMY data sets the max power output predicted was 2866.26 W. The future data set showed a percent increase of maximum power output of 4.33%.

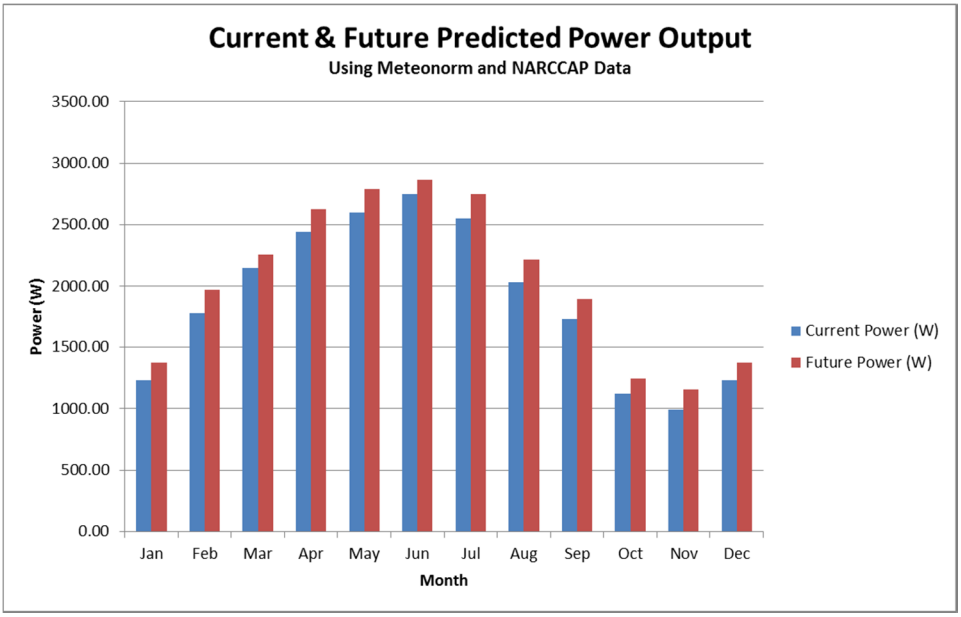

Figure 25. Current and future predicted power output by month using Meteonorm TMY and future TMY data sets.

4.5 Summary and Conclusions

The results of the predicted PV output using the recorded data was compared to the recorded power output of the system. The purchased weather data was compared to the recorded data for use in the TRNSYS simulation. The purchased weather data was used to create a typical meteorological year data set and a future typical meteorological year data set to perform future PV performance predictions. The results of the TRNSYS simulation for predicted future PV performance was presented. The following chapter will discuss the results presented in this chapter and their value in future research.

Chapter 5

Discussion

5.1 Discussion of the Five-Parameter Model Results

Using De Soto's model, the maximum power predicted was 242.63 W per module totaling 8006.89 W for the 33 modules in the system. This prediction is higher than what is given by the manufacturer data sheet of a max power of 225 W per module for a total of 7425 W for the system. De Soto's five-parameter model predicts the power output of the system using data from the manufacturer about the modules at standard test conditions. The five-parameter model does not take into account the weather that the modules are subjected to, nor does it take into account the inverter that this system is connected to. The five-parameter model also neglects losses due to dirt and dust, angular losses, mismatch losses, temperature losses, ohmic losses and losses due to shading. The five-parameter offers a good way to determine the power output of a system if the only thing available is the manufacturer data sheet. Using weather data and, in this case, inverter data the power output can be more accurately predicted.

5.2 Discussion of PV Performance with Recorded Weather Data

5.2.1 Recorded weather data

High temperatures were recorded during the summer months with the lowest temperatures recorded during the winter months. The trend for radiation was similar, though slightly offset by the temperature spikes and divots. Approximately one to two months after the radiation began to increase did the temperature also increase. This is typical of solar radiation and temperature trends. Typically, temperature will lag behind that of incoming solar radiation as the earth attempts to balance incoming and outgoing energy. The values of temperature in the recorded

data set match those presented in the research and methods portion of this paper acquired from the U.S. climate database.

Though wind speed had a large range of data for each month, it was clear that the highest wind speed occurred during the winter months and the coldest temperatures. This is probably due to the cold fronts that happen during the winter months in the area in question. Cold fronts coming from the north typically bring stronger winds attributing to the data presented in the previous chapter.

Due to the typical trend of lag between temperature and radiation, the recorded temperature data matching that of the U.S. climate database and the typical trend of higher wind speeds during the winter months due to cold fronts, it was determined that the recorded data was accurate enough to proceed with simulation runs.

5.2.2 TRNSYS simulation results

The results of the TRNSYS simulation showed a strong correlation between PV performance and radiation, temperature and wind speed with the strongest contributing factor being radiation. The maximum power output was predicted to be 6771 Watts using the recorded data. The maximum power output possible by the solar panels used is 225 Watts as described by the manufacture data sheet per module, totaling 7425 W for the system. Using this information it was predicted that the maximum efficiency for the solar panels was predicted to be 91%. The total radiation recorded was input into the TRNSYS model as beam radiation (TRNSYS uses both beam and diffuse radiation to determine total, with 85% of the total being contributed by beam), therefore the model assumed a less amount of radiation than was available resulting in lower values than the actual output. This accounts for the discrepancy between the predicted performance of 6771 W to the measured performance of 7095 W.

The predicted and recorded power output results were compared using the percentage difference of the root mean square error (RMSE) between the two results. The percent difference between the RMSE's for the predicted and recorded values was -16%. A percent difference of ±5% is what is desired. The reason for the high difference between the predicted and recorded power output results might be attributed to the recorded data for radiation. It was known that there were bad readings for radiation in the recorded data (negative values for radiation were recorded, which is not possible). There were also absent readings of radiation as well as the deleted negative values. The TRNSYS simulation will still run the simulation for no values of radiation and low values of radiation which will result in no or low power outputs. The recorded power output simply recorded the power supplied by the system and was not affected by the radiation recordings. This discrepancy is likely to have caused a difference in the predicted and recorded power output results.

$$RMSE = \sqrt{\frac{1}{N}\sum_{i=1}^{N}(x_i - x'_i)^2} \tag{60}$$

5.3 Discussion of Meteonorm Purchased Data Validation

5.3.1 Purchased weather data

To allow for future performance predictions of the PV system, the method using a typical meteorological year was used. This method involved creating a typical meteorological year using data over a 10 year time frame purchased from Meteonorm and then using the predicted change data from NARCCAP to determine the future typical meteorological year.

The comparisons between the recorded data and the purchased data had varying results. The percent difference between the recorded and purchased data for temperature was an average of 1.31%. It was safe to assume that the average temperature data from Meteonorm was

comparative to the recorded data obtained from the weather station atop TxAIRE House 2. The wind speed data, however, had an average percent difference of 41.53%. Upon review of the data, it was determined that the Meteonorm wind speed data did not include the extreme wind conditions seen by the weather station. The use of wind speed in PV performance models is important because of the effect it has on the temperature of the cell/modules themselves, which has an effect on performance as discussed in chapter 2. The effect of wind speed on the performance of PV modules was discussed by Bhattacharya et al. [80] to have a moderate positive correlation between wind speed and performance. The wind speed and performance for a PV system was recorded for one year and the data was compared. Bhattacharya et al. determined the correlation coefficient (R) for wind speed and performance to be 0.9642 meaning the coefficient of determination (R^2) was 47.02% leaving 52.98% of the total variation to be unexplained. It was determined that because radiation is the greatest factor determining PV performance followed by temperature and then wind speed, and the temperature data being very accurate compared to the recorded data, it was adequate to not use the Meteronorm wind speed data as it did not follow the recorded data closesly.

The radiation data from Meteonorm was adequate in that it followed the trend of the radiation of the recorded data; however the differences between the data caused lower overall power outputs than what was seen with the recorded data leading to lower overall power predictions. The reason for the large difference between radiation can be attributed to the way the data was presented. The radiation data was given by Meteonorm in TMY format, which uses the most typical values from each month over several years. These values do not include maximum and minimum values. The recorded data however, includes all data from the time period including the maximum and minimum values which will result in higher and lower values of

power output. The results of the TRNSYS simulation showed that the Meteonorm data could not be used to accurately represent the PV system. However, the model did provide insight into the leading factor that influences the power output. The temperature averages were relatively the same and wind speed was excluded, this left only radiation to be the main factor in determining PV performance.

5.4 Discussion of PV Performance Using the future TMY

5.4.1 Future TMY

As mentioned previously, the Meteonorm data proved to be inadequate for this research but was continued with and used to create the typical meteorological year to understand the implications of varying data. To determine the future power performance of the system, a future typical meteorological year data set was created using the original Meteonorm TMY and predicted climate change data from NARCCAP. NARCCAP predicted an average temperature increase of 36.11ºF, an average radiation increase of 11.67 $\frac{W}{m^2}$ and an average decrease of wind speed of -.12 mph. This data was used to predict the future performance of the system.

5.4.2 TRNSYS simulation results for future predicted performance

The power output between the current TMY and the future TMY increased by 4% because of the predicted increased radiation. The overall low power outputs can be attributed to the differences in radiation from the recorded data to the Meteonorm data as mentioned previously.

The power output for the current Meteonorm TMY data set showed a max power output of 2747.41 W during the month of June as seen in Figure 25. Using the future TMY data sets the max power output predicted was 2866.26 W. The future data set showed a percent increase of maximum power output of 4.33%. Though the results using Meteonorm proved to be

unacceptable for PV performance, the results from the current TMY to the future TMY did provide additional insight into the factors affecting PV performance.

The results showed that with a 48% increase in temperature and a 9% increase in radiation there was only a 4% increase in overall power output. This information adds more confirmation that radiation has a higher impact on the performance of the system than temperature.

5.5 Limitations and Delimitations

5.5.1 Limitations of the study

There were several limitations to the study and prediction of the PV system in this study. The study was limited in its finding by the following:

- Archival data
    - The TRNSYS software requires the data to be in the same time intervals between the different inputs of temperature, radiation, etc. The data, however, was recorded in several different time intervals and the smallest interval consistent between the inputs was 30 minutes. Therefore, the data points taken in 5 minute increments were not all used and the data had to be modified so that all inputs had the same dates and time intervals.
    - The recorded weather data and PV output data was limited to the amount of data that had been recorded during the years 2012 – 2014. This amount of data was not enough to create TMY data sets for future predictions of the system.
    - Missing data points and bad readings (negative readings for radiation and wind speed) were also a part of the archival data. All of the data had to be examined and the bad readings had to be deleted.

- Though some success has been experienced with weather forecasting predictions, the research is relatively new and solar forecasting has small errors within a few hours, however the further into the future the forecast the higher the error.
- TRNSYS uses radiation data in the form of beam and diffuse radiation to make its calculations, however the measured radiation was of the total radiation on the tilted surface of the PV modules. To run the model, the total radiation was treated as beam radiation (beam radiation typically makes up about 85% of the total radiation).
- The power output predictions in this study can only be used for the Tyler, TX area as the data was either the recorded data recorded at the UT Tyler campus, or from the weather station at the Tyler, TX Pounds Fld airport.

5.5.2 Delimitations of the study

The study was also delimited in its findings by the following:

- The amount of recorded data was limited; therefore data was purchased so that TMY data sets could be developed for power predictions of the system. The TMY data sets purchased did not match the recorded data as closely as expected and produced much lower predicted power output results. Due to time, other outsource companies for weather data were not researched.
- Due to resources in equipment and time, the losses in the system due to dirt and dust, angular losses, losses due to differences with the nominal power, mismatch losses, temperature losses, losses due to monitoring errors of the maximum peak, ohmic losses in cabling, and losses due to shading were not evaluated. These losses would have required more data for evaluation, for example the temperature losses would have required

thermocouples to be placed on the cells to determine temperature which then could have been used to calculate the loss it had on the overall power output.

5.6 Summary and Conclusions

Using recorded data at the site provided a more accurate model than of the data supplied by the outside source, though more time was needed to modify the recorded data for usability with the simulation software. Though daily values for radiation were not available for the area and dates in question, future measurements might be available and using daily values from Meteonorm for radiation will provide a comparative model to using the recorded data at the site. The TRNSYS model proved to under predict the power output by approximately 5% compared to the recorded power output. This model can be used for future research, with varying results dependent on the area in question, with recorded or purchased data rendering the fact that purchased data would need to include a minimum of daily radiation values.

Chapter 6

Conclusions and Recommendations

6.1 Conclusions

This paper reviewed the measured and predicted performance of a photovoltaic grid connected system in a humid subtropical climate. Several models including numerical, experimental and simulation models were researched and discussed. It was determined from the research that a five-parameter, one-diode model was the best model to predict PV performance based on complexity of the model and accuracy. Simulations were modeled using the five-parameter, one-diode in the TRNSYS software package to provide adequate results for PV performance of the grid connected system in question.

The results of this project have shown that in determining the prediction performance of a PV grid connected system the following should be taken into account:

- The weather data has the most significant effect on the prediction performance, with the most effect coming from the radiation data. The actual performance of the system compared to the predicted performance using purchased data yielded an 88% difference while comparing to the predicted performance using the recorded data yielded a 5% difference in the max power output; therefore carefully selecting the correct weather data set is crucial; particularly the radiation data.
- Though recorded data was used, a difference between the recorded power output and the predicted output was still 5%.
- To determine future predicted performance a good radiation data set over a long period of time is needed. The comparison of the typical meteorological year data and the radiation

data from 2012 – 2014 showed an average difference of 31% which causes a large variation in prediction performance.

Though accuracy can be increased with the addition of the losses and additional data for radiation, the model using TRNSYS was determined to provide an accurate model of power performance predictions. This model is simple but accurate and can help to design future PV systems in the East Texas area as well as help to improve current PV systems.

6.2 Recommendations

As mentioned, the data recorded for the simulation was taken using several pieces of equipment with varying time intervals. Due to this, extensive time was needed to modify the data points to sync date and time between the various data sets. To aid in future research, it would be beneficial to set the equipment to record data in the same time intervals if possible. This would allow for quicker results as time would not be needed to review the data as extensively. The data acquired also comprised of invalid readings due to technical issues with the data logger. The readings would show negative values for radiation and/or wind speed or would simply not record any data at all. Since the data received was archival data and the specific reasons for the invalid readings were not recorded at the time of acquiring the data, the reasons for the invalid data points could not be determined. Future research would benefit from determining the cause of the invalid readings at the time of occurrence and work performed to prevent it. Though the data had invalid readings and varying time intervals, the data was able to be modified as shown previously with believable values and trends for the area.

Though the recorded data used showed typical trends and values for the given area, the simulation results for power output still gave a percent difference of 5% between the recorded power data to the predicted data. To achieve a smaller percent difference, and greater accuracy

for the simulation model, including losses due to dirt and dust, angularity, differences with the nominal power, mismatch, monitoring errors of the maximum peak, ohmic losses in cabling and losses due to shading can be taken into account. The addition of these losses will attribute to a more accurate model for future research.

To use the Meteonorm data in future research, the researcher should attempt to reduce the differences between recorded and purchased data by one of two options. The first option would be to capture the extreme data values by finding the maximum and minimum average percent differences by month and using this factor to multiply by the purchased data. This would give a closer representation of the data recorded at the site. Or, the second option would be to only use the average data for temperature and exclude the wind speed data as the average temperature data acquired by Meteonorm was very accurate. These approaches would work for temperature and wind speed; however for radiation it would be the most beneficial to use recorded data as mentioned in the previous chapter or research other sources for more accurate radiation data.

References

[1] U.S Energy Information Administration. 2013 World Energy Consumption. Accessed September, 2014. Retrieved from: http://www.eia.gov/todayinenergy/detail.cfm?id=12251

[2] Shahriar S, Topal E. When will fossil fuels reserves be diminished? Energy Policy 2009; Vol 37: pp 181-189

[3] Alemà-Nava G S, Casiano-Flores V H, Càrdenas-Chàvez D L, Dallemand JF, Parra R. Renewable and Sustainable Energy Reviews 2014; Vol 32: pp 140-153.

[4] Singh G.K. Solar power generation by PV (photovoltaic) tenchnology: A review. Energy 2013; Vol 53: pp 1-13

[5] Devabhaktuni V, Alam M, Depuru SSSR, Green R.C, Nims D, Near C. Solar Energy: Trends and enabling technologies. Renewable and Sustainable Energy Reviews 2013; Vol 19: pp 555-564.

[6] Robert Kropp. 2009. Solar Expected to Maintain its Status as the World's Fastest-Growing Energy Technology. SRI World Group, Inc. Accessed September, 2014. Retrieved from: http://www.socialfunds.com/news/article.cgi/2639.html

[7] Fruanhofer Instistute for Solar Energy Systems ISE. 2014. Photovoltaics Report. Fraunhofer ISE. Accessed November, 2014. Retrieved from: http://www.ise.fraunhofer.de/en/downloads-englisch/pdf-files-englisch/photovoltaics-report-slides.pdf

[8] Mulcué-Nieto LF, Mora-López L. A new model to predict the energy generated by a photovoltaic system connected to the grind in low latitude countries. Solar Energy 2014; Vol 107: pp 423-442.

[9] Almonacid F, Rus C, Pérez-Higueras P, Hontoria L. Calculation of the energy provided by a PV generator. Comparative study: Conventional methods vs. artificial neural networks. Energy 2011; Vol 36: pp 375-384.

[10] Erge† T, V.U Hoffmann, Kiefer K. The german experience with grid-Connected PV-systems. Solar Energy 2001; Vol 70: pp 479-487.

[11] Huld T, Gottschalg R, HG Beyer, Topic M. Mapping the performance of PV modules, effects of module type and data averaging. Solar Energy 2010; Vol 84: pp 324-338.

[12] Tian H, Mancilla-David F, Ellis K, Muljadi E, Jenkins P. A cell-to-module-to-array detailed model for photovoltaic panels. Solar Energy 2012; Vol 86: pp 2695-2706.

[13] Fuentes M, Nofuentes G, Aguilera J, Talavera D.L, Castro M. Application and validation of algebraic methods to predict the behavior of crystalline silicon PV modules in Mediterranean climates. Solar Energy 2007; Vol 81: pp 1396-1408.

[14] Mohanty P, Bhuvaneswari G, Balasubramanian R, Dhaliwal NK. MATLAB based modeling to study the performance of different MPPT techniques used for solar PV system under various operating conditions. Renwable and Sustainable Energy Reviews 2014; Vol 38: pp 581-593.

[15] Paulescu M, Badescu V, Dughir C. New procedure and field-tests to assess photovoltaic module performance. Energy 2014; Vol 70: pp 49-57.

[16] De Soto W, Klein S.A, Beckman W.A. Improvement and validation of a model for photovoltaic array performance. Solar Energy 2006; Vol 80: pp78-88.

[17] ERDEM Z, ERDEM M.B. A Proposed Model of Photovoltaic Module in Matlab/Simulink™ for Distance Education. Procedia – Social and Behavioral Sciences 2013; Vol 103: pp 55-62.

[18] Chouder A, Silvestre S, Sadaoui N, Rahmani L. Modeling and simulation of a grid connected PV system based on the evaluation of main PV module parameters. Simulation Modeling Practice and Theory 2012; Vol 20: pp 46-58.

[19] Kumari J.S, Babu Ch.S. Mathematical Modeling and Simulation of Photovoltaic Cell using Matlab-Simulink Environment In:International Journal of Electrical and Computer Engineering (IJECE) 2012; Vol 2: pp 26-34.

[20] Ishaque K, Salam Z, Syafaruddin. A comprehensive MATLAB Simulink PV system simulator with partial shading capability based on two-diode model. Solar Energy 2011; Vol 85: pp 2217-2227.

[21] Ma T, Yang H. Lu L. Solar photovoltaic system modeling and performance prediction. Renewable and Sustainable Energy Reivews 2014; Vol 36: pp 304-315.

[22] Krismadinata, Rahim N.Abd, Ping HW, Selvaraj J, Photovoltaic module modeling using simulink/matlab. Procedia Environmental Sciences 2013; Vol 17: pp 537-546.

[23] Qi C, Ming Z. Photovoltaic Module Simulink Model for a Stand-alone PV System. Physics Procedia 2012; Vol 24: pp 94-100.

[24] Celik AN, Acikgoz N. Modelling and experimental verification of the operating current of mono-crystalline photovoltaic modules using four- and five-parameter models. Applied Energy 2007; Vol 84: pp 1-15.

[25] Amad G.E, Hussein H.M.S, El-Ghetany H.H. Theoretical analysis and experimental verification of PV modules. Renewable Energy 2003; Vol 28: pp 1159-1168.

[26] Karamirad M, Omid M, Alimardani R, Mousazadeh H, Heidari SN. Theoretical analysis and experimental verification of PV modules. Simulation Modelling Practice and Theory 2013;Vol 34: pp 86-98.

[27] Khatib T, Sopian K, Kazem HA. Actual performance and characteristic of a grid connected photovoltaic power system in the tropics: A short term evaluation. Energy Conversion and Management 2013; Vol 71: pp 115-119.

[28] Singh G.K. Solar power generation by PV (photovoltaic) technology: A review. Energy 2013; Vol 53: pp 1-13.

[29] Ma T, Yang H, Lu L. Development of a model to simulate the performance characteristics of crystalline silicon photovoltaic modules/strings/arrays. Solar Energy 2014; Vol 100: pp 31-41.

[30] Bai J, Liu S, Hao Y, Zhang Z, Jiang M, Zhang Y. Development of a new compound method to extract the five parameters of PV modules. Energy Conversion and Management 2014; Vol 79: pp 294-303.

[31] Lo Brano V, Orioli A, Ciulla G. On the experimental validation of an improved five-parameter modelfor silicon photovoltaic modules. Solar Energy Materials & Solar Cells 2012; Vol 105: pp 27-39.

[32] Jung JH, Ahmed S. Real-time simulation model development of single crystalline photovoltaic panels using fast computation methods. Solar Energy 2012; Vol 86: pp 1826-1837.

[33] Iero D, Carbone R, Carotenuto R, Felini C, Merenda M, Pangallo G, Corte FGD. SPICE modelling of a complete photovoltaic system including modules, energy storage elements and a multilevel inverter. Solar Energy 2014; Vol 107: pp 338-350.

[34] Lo Brano V, Ciulla G. An efficient analytical approach for obtaining a five parameters model of photovoltaic modules using only reference data. Applied Energy 2013; Vol 111: pp 894-903.

[35] de Blas M.A, Torres J.L, Prieto E, Garcia A. Selecting a suitable model for characterizing photovoltaic devices. Renewable Energy 2002; Vol 25: pp 371-380.

[36] Pathak M.J.M, Sanders P.G, Pearce J.M. Optimizing limited solar roof access by exergy analysis of solar thermal, photovoltaic, and hybrid photovoltaic thermal systems. Applied Energy 2014; Vol 120: pp 115-124.

[37] Lo Brano V, Orioli A, Ciulla G, Di Gangi A, An improved five-parameter model for photovoltaic modules. Solar Energy Materials & Solar Cells 2010; Vol 94: pp 1358-1370.

[38] Ayompe L.M, Duffy A, McCormack S.J, Conlon M. Validated real-time energy models for small-scale grid-connected PV-systems. Energy 2010; Vol 35: pp 4086-4091.

[39] Chouder A, Silvestre S, Taghezouit B, Karatepe E. Monitoring, modelling and simulation of PV systems using LabVIEW. Solar Energy 2013; Vol 91: pp 337-349.

[40] Demain C, Journée M, Bertrand C. Evaluation of different models to estimate the global solar radiation on inclined surfaces. Renewable Energy 2013; Vol 50: pp 710-721.

[41] Baltus C.W.A, Eikelboom J.A, van Zoliingen R.J.C. Analytical monitoring of losses in PV systems. Paper presented at the 14th European Photovoltaic Solar Energy Conference Barcelona, 30 June - 4 July 1997.

[42] Ueda Y, Kurokawa K, Kitamura K, Yokota M, Akanuma K, Sugihara H. Performance analysis of various system configurations on grid-connected residential PV systems. Solar Energy Materials & Solar Cells 2009; Vol 93: pp 945-949.

[43] Drif M, Pérez P.J, Aguilera J, Almonacid G, Gomez P, de la Casa J, Aguilar J.D. Univer Project. A grid connected photovoltaic system of 200kWp at Jaén University. Overview and performance analysis. Solar Energy Materials & Solar Cells 2007; Vol 91: pp 670-683.

[44] Sarver T, Al-Qaraghuli A, Kazmerski L.L. A comprehensive review of the impact of dust on the use of solar energy: History, investigations, results, literature, and mitigation approaches. Renewable and Sustainable Energy Reviews 2013; Vol 22: pp 698-733.

[45] Marion B, Adelstein J, Boyle K, Haden H, Hammond B, Fletcher T, Canada B, Narang D, Shugar D, Wenger H, Kimber A, Mitchell L, Rich G, Townsend T. Performance Paramters for Grid Connected PV Systems. Paper presented at the 31st IEEE Photovoltaics Specialists Conference and Exhibition, Florida, January 3-7 2005.

[46] Rodrigo P, Rus C, Almonacid F, Pérez-Higueras P.J, Almonacid G. A new method for estimating angular, spectral and low irradiance losses in photovoltaic systems using an artificial neural network model in combination with the Osterwald model. Solar Energy Materials & Solar Cells 2012; Vol 96: pp 186-194.

[47] Martin N, Ruiz J.M. Calculation of the PV modules angular losses under field conditions by means of an analytical model. Solar Energy Materials & Solar Cells 2001; Vol 70: pp 25-38.

[48] Choulder A, Silvestre S. Analysis Model of Mismatch Power Losses in PV Systems. Journal of Solar Energy Engineering 2009; Vol 131: 024504-5.

[49] Wurster T.S, Schubert M.B, Mismatch loss in photovoltaic systems. Solar Energy 2014; Vol 105: pp 505-511.

[50] Skoplaki E, Palyvos J.A. Operating temperature of photovoltaic modules: A survey of pertinent correlations. Renewable Energy 2009; Vol 34: pp 23-29.

[51] Baltus C.W.A, Eikelboom J.A, van Zoliingen R.J.C. Analytical monitoring of losses in PV systems. Paper presented at the 14th European Photovoltaic Solar Energy Conference Barcelona, 30 June - 4 July 1997.

[52] Cullura M, Di Gangi A, Orioli A. A photographic method to estimate the shading effect of obstructions. Solar Energy 2012; Vol 86: pp 886-902.

[53] Yoon K, Yun G, Jeon J, Kim K.S. Evaluation of hourly solar radiation on inclined surfaces at Seoul by Photographical Method. Solar Energy 2014; Vol 100: pp 203-216.

[54] Su Y, Chan L, Shu L, Tsui K. Real-time prediction models for output power and efficiency of grid-connected solar photovoltaic systems. Applied Energy 2012; Vol 93: pp 319-326.

[55] Tawanda Hove. A method for predicting long-term average performance of photovoltaic systems. Renewable Energy 2000; Vol 21: pp 207-229.

[56] Gordon J.M, Zoglin P. A method for predicting long-term average performance of photovoltaic systems. Solar Cells 1986; Vol 17: pp 285-301.

[57] Lam K.H, Lai T.M, To W.M. The application of dynamic modelling techniques to the grid-connected PV (photovoltaic) systems. Energy 2012; Vol 46: pp 254-274.

[58] Durisch W, Bitnar B, Mayor J, Kiess H, Lam K.H, Close J. Efficiency model for photovoltaic modules and demonstration of its application to energy yield estimation. Solar Energy Materials & Solar Cells 2007; Vol 91: pp 79-84.

[59] Rampinelli G.A, Krenzinger A, Romero F.C. Mathematical models for efficiency of inverters used in grid connected photovoltaic systems. Renewable and Sustainable Energy Reviews 2014; Vol 34: pp 578-587.

[60] Thevenard D, Pelland S. Estimating the uncertainty in long-term photovoltaic yield predictions. Solar Energy 2013; Vol 91: pp 432-445.

[61] Al-Sabounchi A.M, Yalyali S.A, Al-Thani H.A. Design and performance evaluation of a photovoltaic grid-connected system in hot weather conditions. Renewable Energy 2013; Vol 53: pp 71-78.

[62] Meyer E.L, van Dyk E.E. Development of energy model based on total daily irradiation and maximum ambient temperature. Renewable Energy 2000; Vol 21: pp 37-47.

[63] Illanes R. De Francisco A, Núñez F, De Blas M, García A, Torres J.L. Dynamic simulation and modelling of stand-alone PV systems by using state equations and numerical integration methods. Applied Energy 2014; Vol 135: pp 440-449.

[64] Pavan A.M, Mellit A, Lughi V. Explicit empirical model for general photovoltaic devices: Experimental validation at maximum power point. Solar Energy 2014; Vol 101: pp 105-116.

[65] Mondol J.D, Yohanis Y.G, Norton B. Solar radiation modelling for the simulation of photovoltaic systems. Renewable Energy 2008; Vol 33: pp 1109-1120.

[66] J.A del Cueto. Comparison of Energy Production and Performance from Flat-Plate Photovoltaic Module Technologies Deployed at Fixed Tilt. Paper presented at the 29th IEEE PV Specialists Conference. New Orleans, Louisiana. May 20-24. 2002.

[67] Cañete C, Carretero J, Sildrach-de-Cardona M. Energy performance of different photovoltaic module technologies under outdoor conditions. Energy 2014; Vol 65: pp 295-302.

[68] Ketjoy N, Sirisamphanwong C, Khaosaad N. Performance Evaluation of 10kWp Photovoltaic Power Generator Under Hot Climatic Condition. Energy Procedia 2013; Vol 34: pp 291-297.

[69] So J.H, Jung Y.S, Yu G.J, Choi J.Y, Choi J.H. Performance results and analysis of 3kW grid-connected PV systems. Renewable Energy 2007; Vol 32: pp 1858-1872.

[70] Vikrant Sharma and S.S Chandel. Performance analysis of a 190 kWp grid interactive solar photovoltaic power plant in India. Energy 2013; Vol 55: pp 476-485.

[71] Mondol J.D, Yohanis Y.G, Norton B. Comparison of measured and predicted long term performance of grid a connected photovoltaic system. Energy Conversion and Management 2007; Vol 48: pp 1065-1080.

[72] Choi Y, Rayl J, Tammineedi C, Brownson J.R.S. PV Analyst: Coupling ArcGIS with TRNSYS to assess distributed photovoltaic potential in urban areas. Solar Energy 2011; Vol 85: pp 2924-2939.

[73] Axaopoulos P.J, Fylladitakis E.D, Gkarakis K. Accuracy analysis of software for the estimation and planning of photovoltaic installations. Int J Energy Environ Eng 2014; Vol 5: pp 71-79.

[74] Trillo-Montero D, Santiago I, Luna-Rodriguez J.J, Real-Calvo R. Development of a software application to evaluate the performance and energy losses of grid-connected photovoltaic systems. Energy Conversion and Management 2014; Vol 81: pp 144-159.

[75] Patton, Shannon. Development of a future typical meteorological year with application to building energy use. Graduate Theses and Dissertations. 2013.

[76] Rich H. Inman, Hugo T.C. Pedro, Carlos F.M. Coimbra. Solar forecasting methods for renewable energy integration. Progress in Energy and Combustion Science 2013; Vol 39: pp 535-576.

[77] Patrick Mathiesen, Jan Kleissl. Evaluation of numerical weather prediction for intra-day solar forecasting in the continental United States. Solar Energy 2011; Vol 85: pp 967-977.

[78] Quesada B, Sánchez C, Cañada J, Royo R, Payã J. Experimental results and simulation with TRNSYS of a 7.2 kWp grid-connected photovoltaic system. Applied Energy 2011; Vol 88: pp 1772-1783.

[79] Mearns, L. O., W. J. Gutowski, R. Jones, L.-Y. Leung, S. McGinnis, A. M. B. Nunes, and Y. Qian: A regional climate change assessment program for North America. EOS (2009) Vol 90: pp. 311-312.

[80] Tanima Bhattacharya, Ajoy K. Chakraborty, and Kaushik Pal: Effects of ambient temperature and wind speed on performance of monocrystalline solar photovoltaic module in Tripura, India. Journal of Solar Energy, Vol. 2014, Article ID 817078, 9 July 2014.

Appendix A. Manufacturer Data Sheet for Solar Panels

Figure A-1 shows the manufacturer data sheet for the solar panels used in this study.

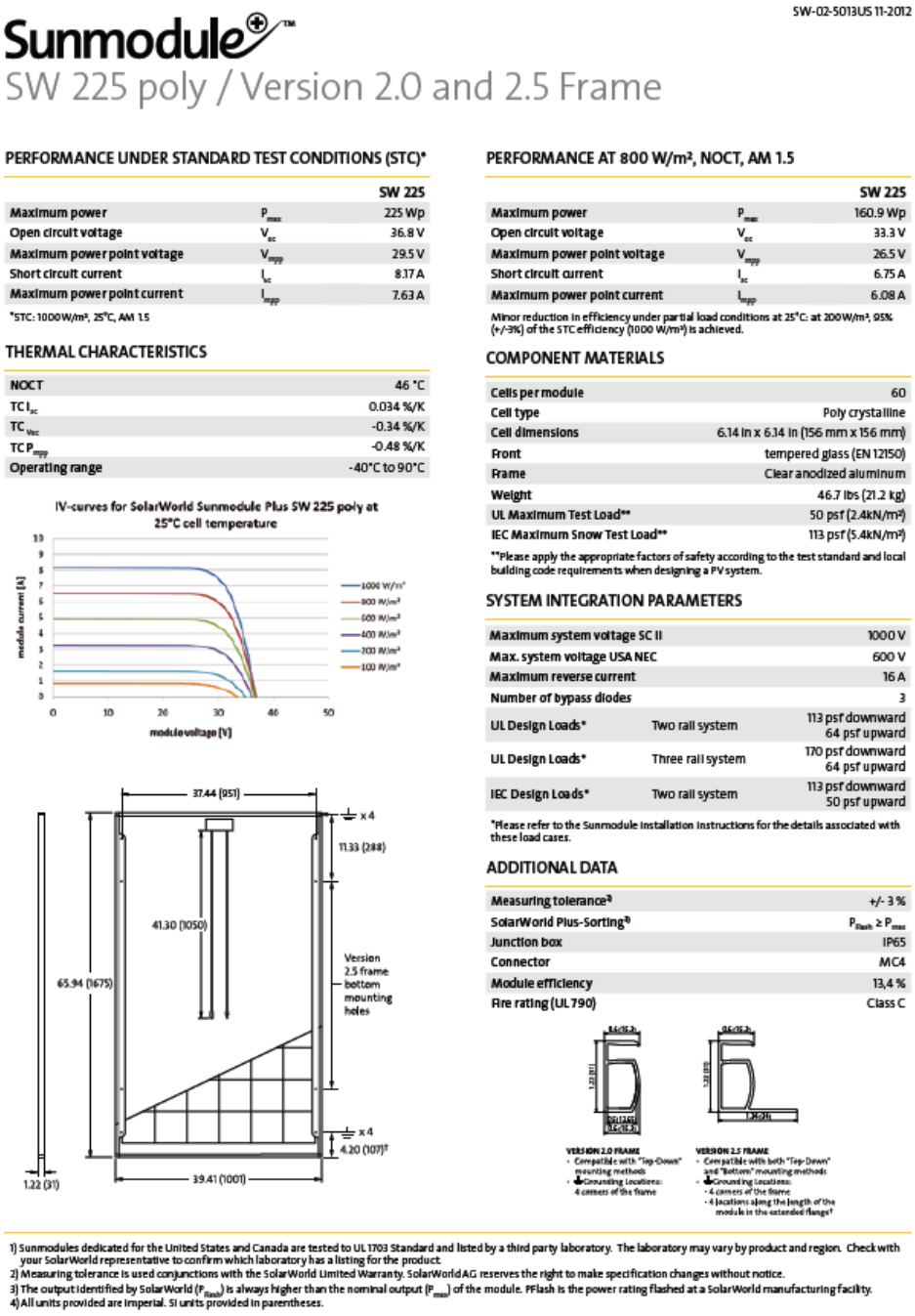

SW-02-5013US 11-2012

Sunmodule™

SW 225 poly / Version 2.0 and 2.5 Frame

PERFORMANCE UNDER STANDARD TEST CONDITIONS (STC)*

		SW 225
Maximum power	P_{max}	225 Wp
Open circuit voltage	V_{oc}	36.8 V
Maximum power point voltage	V_{mpp}	29.5 V
Short circuit current	I_{sc}	8.17 A
Maximum power point current	I_{mpp}	7.63 A

*STC: 1000 W/m², 25°C, AM 1.5

THERMAL CHARACTERISTICS

NOCT	46 °C
TC I_{sc}	0.034 %/K
TC V_{oc}	-0.34 %/K
TC P_{mpp}	-0.48 %/K
Operating range	-40°C to 90°C

IV-curves for SolarWorld Sunmodule Plus SW 225 poly at 25°C cell temperature

PERFORMANCE AT 800 W/m², NOCT, AM 1.5

		SW 225
Maximum power	P_{max}	160.9 Wp
Open circuit voltage	V_{oc}	33.3 V
Maximum power point voltage	V_{mpp}	26.5 V
Short circuit current	I_{sc}	6.75 A
Maximum power point current	I_{mpp}	6.08 A

Minor reduction in efficiency under partial load conditions at 25°C: at 200 W/m², 95% (+/-3%) of the STC efficiency (1000 W/m²) is achieved.

COMPONENT MATERIALS

Cells per module	60
Cell type	Poly crystalline
Cell dimensions	6.14 in x 6.14 in (156 mm x 156 mm)
Front	tempered glass (EN 12150)
Frame	Clear anodized aluminum
Weight	46.7 lbs (21.2 kg)
UL Maximum Test Load**	50 psf (2.4kN/m²)
IEC Maximum Snow Test Load**	113 psf (5.4kN/m²)

**Please apply the appropriate factors of safety according to the test standard and local building code requirements when designing a PV system.

SYSTEM INTEGRATION PARAMETERS

Maximum system voltage SC II		1000 V
Max. system voltage USA NEC		600 V
Maximum reverse current		16 A
Number of bypass diodes		3
UL Design Loads*	Two rail system	113 psf downward 64 psf upward
UL Design Loads*	Three rail system	170 psf downward 64 psf upward
IEC Design Loads*	Two rail system	113 psf downward 50 psf upward

*Please refer to the Sunmodule installation instructions for the details associated with these load cases.

ADDITIONAL DATA

Measuring tolerance[3]	+/- 3 %
SolarWorld Plus-Sorting[3]	$P_{Flash} \geq P_{max}$
Junction box	IP65
Connector	MC4
Module efficiency	13,4 %
Fire rating (UL 790)	Class C

VERSION 2.0 FRAME
- Compatible with "Top-Down" mounting methods
- Grounding Locations: 4 corners of the frame

VERSION 2.5 FRAME
- Compatible with both "Top-Down" and "Bottom" mounting methods
- Grounding Locations:
  - 4 corners of the frame
  - 4 locations along the length of the module in the extended flange[4]

1) Sunmodules dedicated for the United States and Canada are tested to UL 1703 Standard and listed by a third party laboratory. The laboratory may vary by product and region. Check with your SolarWorld representative to confirm which laboratory has a listing for the product.
2) Measuring tolerance is used conjunctions with the SolarWorld Limited Warranty. SolarWorld AG reserves the right to make specification changes without notice.
3) The output identified by SolarWorld (P_{Flash}) is always higher than the nominal output (P_{max}) of the module. PFlash is the power rating flashed at a SolarWorld manufacturing facility.
4) All units provided are imperial. SI units provided in parentheses.

Figure A-1. SunModule SW 225 poly manufacturer data sheet.

Appendix B. Manufacturer Data Sheet for Inverter

Figure B-1 shows the manufacturer data sheet for the inverter used in this study, Sunny Boy 7000-US.

Technical data	Sunny Boy 5000-US			Sunny Boy 6000-US			Sunny Boy 7000-US			Sunny Boy 8000-US	
	208 V AC	240 V AC	277 V AC	208 V AC	240 V AC	277 V AC	208 V AC	240 V AC	277 V AC	240 V AC	277 V AC
Input (DC)											
Max. recommended PV power (@ module STC)	6250 W			7500 W			8750 W			10000 W	
Max. DC power (@ cos φ = 1)	5300 W			6350 W			7400 W			8600 W	
Max. DC voltage	600 V			600 V			600 V			600 V	
DC nominal voltage	310 V			310 V			310 V			345 V	
MPP voltage range	250 V – 480 V			250 V – 480 V			250 V – 480 V			300 V – 480 V	
Min. DC voltage / start voltage	250 V / 300 V			250 V / 300 V			250 V / 300 V			300 V / 365 V	
Max. input current / per string (at DC disconnect)	21 A / 20 A 36 A @ combined terminal			25 A / 20 A 36 A @ combined terminal			30 A / 20 A 36 A @ combined terminal			30 A / 20 A 36 A @ combined terminal	
Number of MPP trackers / fused strings per MPP tracker	1 / 4 (DC disconnect)										
Output (AC)											
AC nominal power	5000 W			6000 W			7000 W			7680 W	8000 W
Max. AC apparent power	5000 VA			6000 VA			7000 VA			7680 VA	8000 VA
Nominal AC voltage / adjustable	208 V / ●	240 V / ●	277 V / ●	208 V / ●	240 V / ●	277 V / ●	208 V / ●	240 V / ●	277 V / ●	240 V / ●	277 V / ●
AC voltage range	183 – 229 V	211 – 264 V	244 – 305 V	183 – 229 V	211 – 264 V	244 – 305 V	183 – 229 V	211 – 264 V	244 – 305 V	211 – 264 V	244 – 305 V
AC grid frequency; range	60 Hz; 59.3 – 60.5 Hz			60 Hz; 59.3 – 60.5 Hz			60 Hz; 59.3 – 60.5 Hz			60 Hz; 59.3 – 60.5 Hz	
Max. output current	24 A	21 A	18 A	29 A	25 A	22 A	34 A	29 A	25 A	32 A	29 A
Power factor (cos φ)	1			1			1			1	
Phase conductors / connection phases	1 / 2	1 / 2	1 / 1	1 / 2	1 / 2	1 / 1	1 / 2	1 / 2	1 / 1	1 / 2	1 / 1
Harmonics	< 4%			< 4%			< 4%			< 4%	
Efficiency											
Max. efficiency	96.7%	96.8%	96.8%	96.9%	96.8%	97.0%	97.1%	96.9%	97.0%	96.3%	96.5%
CEC efficiency	95.5%	95.5%	95.5%	95.5%	95.5%	96.0%	95.5%	96.0%	96.0%	96.0%	96.0%
Protection devices											
DC reverse-polarity protection	●			●			●			●	
Integrated AFCI*	○			○			○			○	
AC short circuit protection	●			●			●			●	
Galvanically isolated / all-pole sensitive monitoring unit	●/–			●/–			●/–			●/–	
Protection class / overvoltage category	I / III			I / III			I / III			I / III	
General data											
Dimensions (W / H / D) in mm (in)	470 / 615 / 240 (18.5 / 24 / 9)										
DC Disconnect dimensions (W / H / D) in mm (in)	187 / 297 / 190 (7 / 12 / 7.5)										
Packing dimensions (W / H / D) in mm (in)	390 / 580 / 800 (16 / 23 / 31.5)										
DC Disconnect packing dimensions (W / H / D) in mm (in)	370 / 240 / 280 (15 / 9 / 11)										
Weight / DC Disconnect weight	64 kg (141 lb) / 3.5 kg (8 lb)									66 kg (145 lb) / 3.5 kg (8 lb)	
Packing weight / DC Disconnect packing weight	67 kg (147 lb) / 4 kg (9 lb)									69 kg (152 lb) / 4 kg (9 lb)	
Operating temperature range (full power)**	–25 °C ... +45 °C (–13 °F ... +113 °F)										
Noise emission (typical)	44 dB(A)			45 dB(A)			46 dB(A)			49 dB(A)	
Internal consumption at night	0.1 W			0.1 W			0.1 W			0.1 W	
Topology	LF transformer			LF transformer			LF transformer			LF transformer	
Cooling concept	OptiCool			OptiCool			OptiCool			OptiCool	
Electronics protection rating / connection area	NEMA 3R / NEMA 3R			NEMA 3R / NEMA 3R			NEMA 3R / NEMA 3R			NEMA 3R / NEMA 3R	
Features											
Display: text line / graphic	●/–			●/–			●/–			●/–	
Interfaces: RS485 / Bluetooth®	o/o			o/o			o/o			o/o	
Warranty: 10 / 15 / 20 years	●/o/o			●/o/o			●/o/o			●/o/o	
Certificates and permits (more available on request)	UL1741 (Second Ed.), UL1998, UL1699B, IEEE 1547, FCC Part 15 (Class A & B), CSA C22.2 No. 107.1-2001										

*For AFCI functionality specify SBXXXXUS-12 when ordering.

**For extended operating temperature range to -40 °C (-40 °F), specify SBXXXXUS-11 or SBXXXXUS-12 when ordering.

● Standard features o Optional features – Not available Data at nominal conditions NOTE: US inverters ship with gray lids.

Type designation	SB 5000US	SB 6000US	SB 7000US	SB 8000US

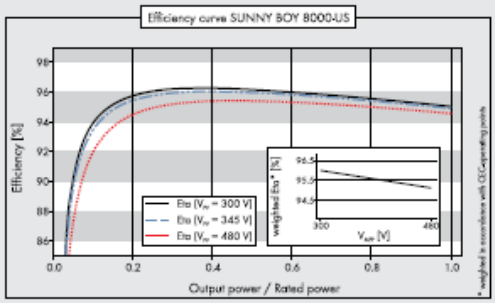

Accessories

RS485 interface
485USPB-NR

Bluetooth Piggy-Back
BTPBINV-NR
with External Antenna
BTPB-EXTANT-NR

Combi-Switch
DC disconnect and PV array combiner box
COMBO-SWITCH

Combiner Box
Simplify wiring for added convenience and safety
SBCB-6-3R or SBCB-6-4

SMA Power Balancer Set
PBL-SBUS-10-NR

Toll Free +1 877 506 1756
www.SMA-Canada.ca

SMA Canada, Inc.

Figure B - 1. Sunny Boy 7000-US manufacturer data sheet.

Appendix C. Formatting the Weather and PV Data

As mentioned in the paper, the data had to be formatted before it could be input into the TRNSYS software. The data was separated in excel files by quarter and separated by weather data and data recorded from the house. The following is an outline in how the data was formatted.

1. Copy the date, time and radiation data from each house excel file and place into one excel file for the total years.
2. Copy the date, time, outside temperature and wind speed data from each weather excel file and place into another excel file for the total years.
3. Figure C - 1 and Figure C - 2 show an example of the house and weather compiled raw data, respectively, from the beginning of the recorded data. As shown, the data for the house started on 5/8/2012 and began recording every 5 minutes. The weather data didn't start recording until 5/25/2012 and recorded every 30 minutes except at some points, for example the first to second data point has a 10 minute interval.

	A	B	C
1	Date	Time	22
2	5/8/2012	10:00:00 AM	1325.88
3	5/8/2012	10:05:00 AM	1327.26
4	5/8/2012	10:10:00 AM	1336.32
5	5/8/2012	10:15:00 AM	1352.1
6	5/8/2012	10:20:00 AM	1361.16
7	5/8/2012	10:25:00 AM	1371.6
8	5/8/2012	10:30:00 AM	1370.64
9	5/8/2012	10:35:00 AM	1375.56
10	5/8/2012	10:40:00 AM	1375.38
11	5/8/2012	10:45:00 AM	1360.56
12	5/8/2012	10:50:00 AM	1365.9
13	5/8/2012	10:55:00 AM	1373.4
14	5/8/2012	11:00:00 AM	1383.84
15	5/8/2012	11:05:00 AM	1392.3

Figure C - 1. House compiled raw data.

	A	B	C	D
1	Date	Time	Temp Out	Wind Speed
2	5/25/2012	9:20:00 AM		0
3	5/25/2012	9:30:00 AM	78	6
4	5/25/2012	10:00:00 AM	79.2	6
5	5/25/2012	10:30:00 AM	80.7	7
6	5/25/2012	11:00:00 AM	81.1	6
7	5/25/2012	11:30:00 AM	82.2	6
8	5/25/2012	12:00:00 PM	83.1	6
9	5/25/2012	12:30:00 PM	84.3	7
10	5/25/2012	1:00:00 PM	86.1	5
11	5/25/2012	1:30:00 PM	87.2	5
12	5/25/2012	2:00:00 PM	88.4	5
13	5/25/2012	2:30:00 PM	88.7	7
14	5/25/2012	3:00:00 PM	89.5	6
15	5/25/2012	3:30:00 PM	90.2	5

Figure C - 2. Weather compiled raw data.

4. In order to segregate the 30 minute data points, each time cell was divided by 0:30 minutes in a separate column as shown in Figure C - 3. The cells in column C had to be formatted into general numbers (Right-click, Format cells, Number, click on general) to give numbers in decimal format instead of time. Time in 30 minute increments would result in whole numbers.

	A	B	C	D	E	F
1	H2-Date	H2-Time		Total Solar Radiation on PV Collectors (22)		
2	10/01/2014	12:30:00 AM	=B2/F2	8.7114		0:30
3	10/01/2014	1:00:00 AM	2	8.1198		

Figure C - 3. Example of time cell divided by 0:30 minutes.

5. Another column was added after column C to differentiate between the whole numbers and the decimals. In column C, the following equation was used =INT(C2)=C2. If the number in the C column was an integer it would return “TRUE” in column D, otherwise it would return “FALSE”.
6. The “FALSE” numbers were filtered out and deleted leaving only the time values in 30 minute increments. Columns C and D were then deleted.
7. Steps 4 – 6 were repeated for the entire data set and added to a master excel sheet of all the data.
8. The entire data set was then reviewed to make sure the dates matched between the house and weather data. If there was missing data in one or the other, empty cells were added so that the date and time were consistent. Figure C - 4 shows an example of some of the finished data with empty cells for unrecorded times.

	A	B	C	D	E	F
1	Date	Time	Total Solar Radiation on PV Collectors (22)	Temp Out	Wind Speed	Outside Humidity
7197	11/8/2012	12:00:00 PM	534.402	68	4	47
7198	11/8/2012	12:30:00 PM	531.84	69.6	4	49
7199	11/8/2012	1:00:00 PM	535.386	71.3	6	48
7200	11/8/2012	1:30:00 PM	532.632	72.3	4	49
7201	11/8/2012	2:00:00 PM	532.824	73	5	48
7202	11/8/2012	2:30:00 PM	538.932	73.7	4	48
7203	11/8/2012	3:00:00 PM	528.69	74.1	5	49
7204	11/8/2012	3:30:00 PM		73.8	4	50
7205	11/8/2012	4:00:00 PM		73.4	3	52
7206	11/8/2012	4:30:00 PM		72.7	2	54
7207	11/8/2012	5:00:00 PM		70.2	1	58

Figure C - 4. Example of data formatting with empty cells.

9. The last step was to convert the date and time formats. The date had to be converted to day of the year only, and the time had to be converted to decimal format.
10. To change the date, the following equation was used =A1-DATE(YEAR)(A1),1,1)+1 to convert the date format to day of the year as shown in Figure C - 5.

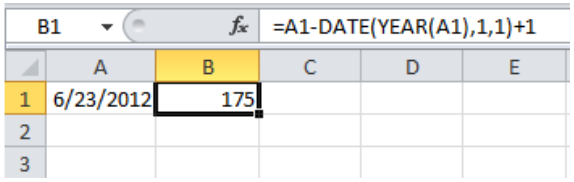

Figure C - 5. Equation to convert date format to day of the year.

11. To convert the time to decimal format, each time cell was multiplied by 24.
12. An example of the finished formatted data is shown in Figure C - 6.

	A	B	C	D	E
1	Date (Day of the Year)	Time (Time of the Day)	Incident Radiation on Tilted Surface (W/m^2)	Temp Out (°F)	Wind Speed (mph)
2	229	24		83	0
3	229	1		82.5	1
4	229	1.5		81.9	0
5	229	2		81	0
6	229	3		81.6	0
7	229	4.5		71.1	5
8	229	5.5		70.6	3
9	229	6		70.3	5
10	229	6.5		71.5	6
11	229	7		69.2	4
12	229	7.5		69.2	3
13	229	8	1.4208	70.2	3
14	229	8.5	1.02684	70.6	4
15	229	9	1.02684	70.3	2
16	229	9.5	0.82968	69.8	4
17	229	10	33.3408	70	1
18	229	10.5	115.704		
19	229	11	83.19	71.1	0

Figure C - 6. Example of finished formatted data.

Appendix D. Using the TRNSYS Software to Predict PV Performance

The following is a guideline on using the TRNSYS software package to predict PV performance using the data as described in the study and formatted as shown in Appendix C.

1. Components used: Controller (2), Type9 (1), Type194b (1) and Type65d (1).
2. Controller 1 (labeled “Start and Stop Times”) was used to give the start and stop times of the simulation. Figure D - 1 shows the window for the calculator and how it was used. Three variables were created: START_TIME, INTERVAL and STOP_TIME. Each was given a value, as shown. The start time and stop time are input into this component in terms of hours of the year. For example, if the data file starts on the 145th day of the year at midnight, then the input for start time would be 3480 (24 * 145). The interval is the amount of data points in the weather data file. The stop time is the interval number added to the start time number.

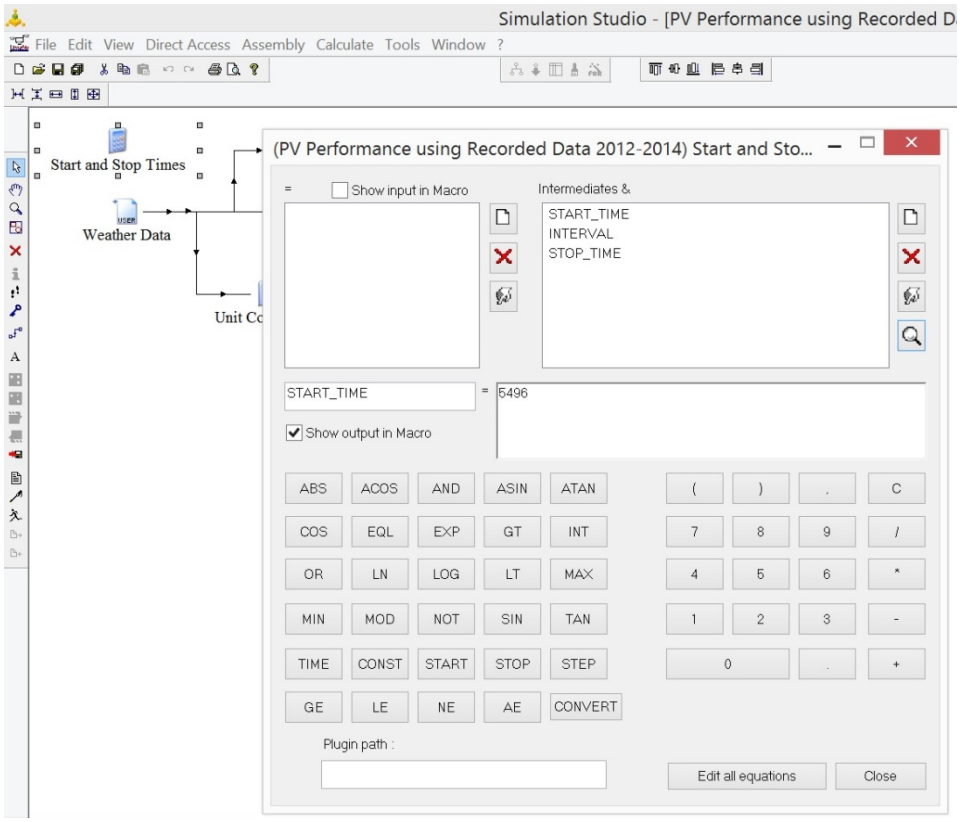

Figure D - 1. Controller 1 parameter window.

3. Type9 (labeled “Weather Data”) was used to read the recorded weather data. Figure D - 2 shows the parameter window for this component.

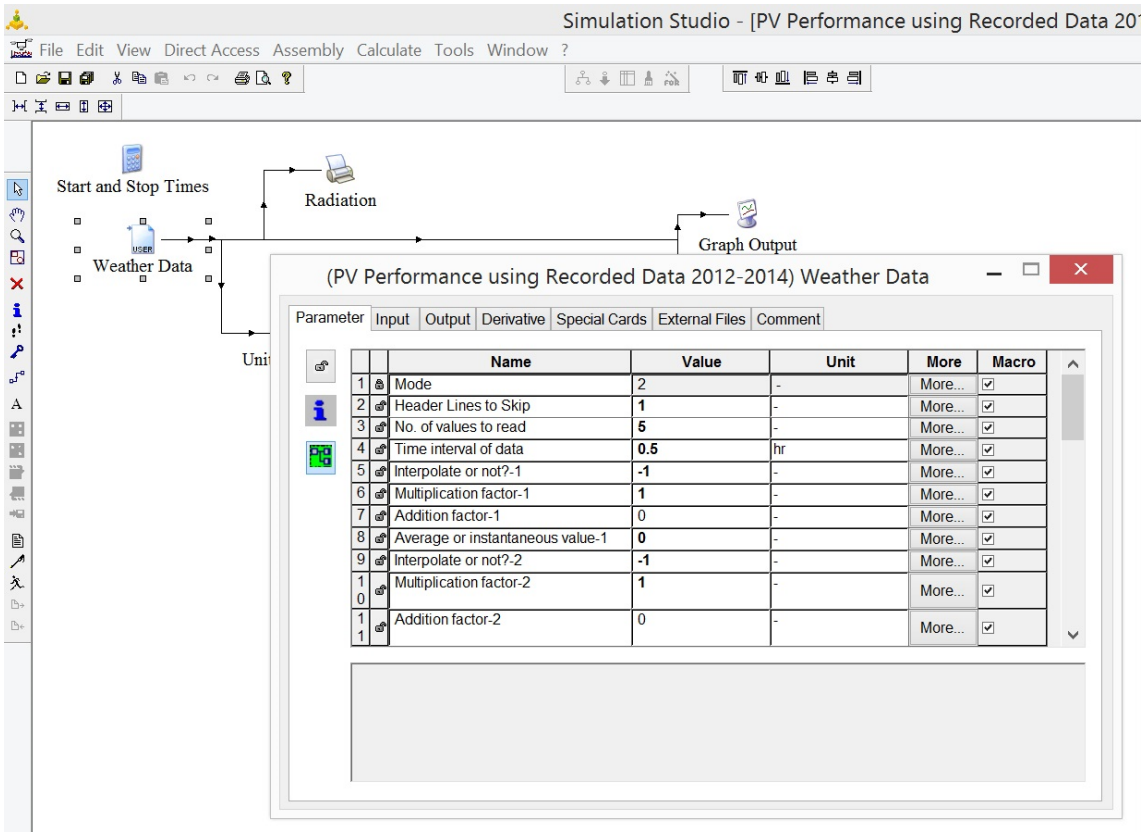

Figure D - 2. Weather Data parameter window.

a. The mode used was 2 (1 uses only instantaneous values while 2 uses both instantaneous and averaged values).
b. The weather data file used had one header line for the name of each characteristic therefore 1 was input into the second parameter.
c. Five sets of columns are in use in the file, therefore 5 was input into the third parameter. All other parameters were left as default
d. To input the weather data file, the tab labeled External Files was clicked and the weather data file was input as shown in Figure D - 3.

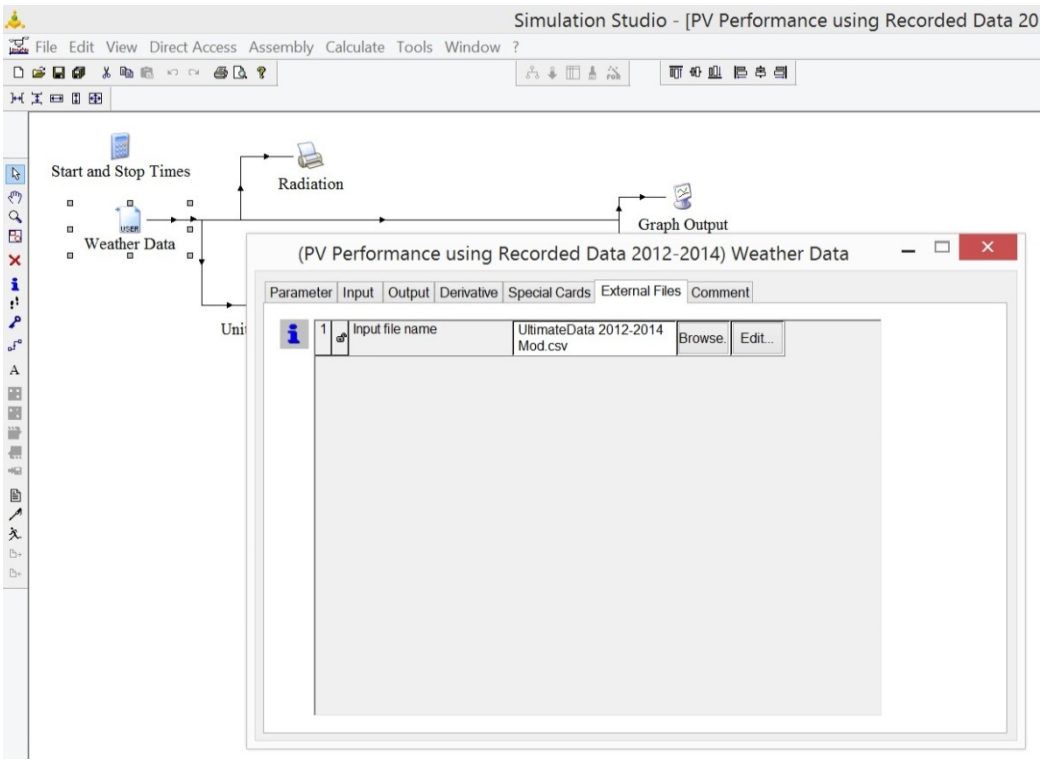

Figure D - 3. Weather Data input window.

e. Figure D - 4 shows the connections between the outputs of Type9 into the input of Controller 2 (labeled “Unit Conversion”).

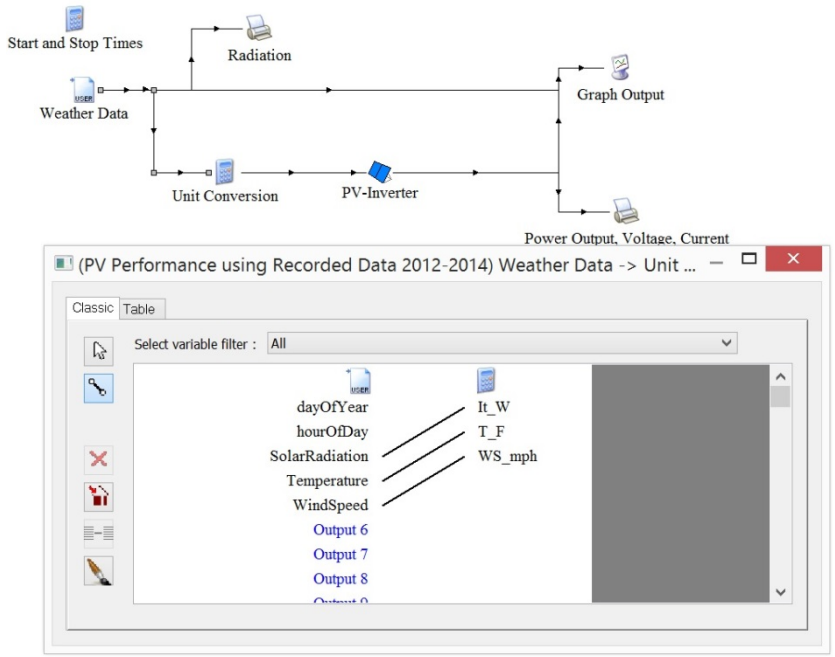

Figure D - 4. Connections between Type9 and Controller 2.

4. Controller 2 was used to convert the weather data units into SI units.
    a. The equations for W to kJ, F to C and mph to ms were used as shown in Figure D - 5.

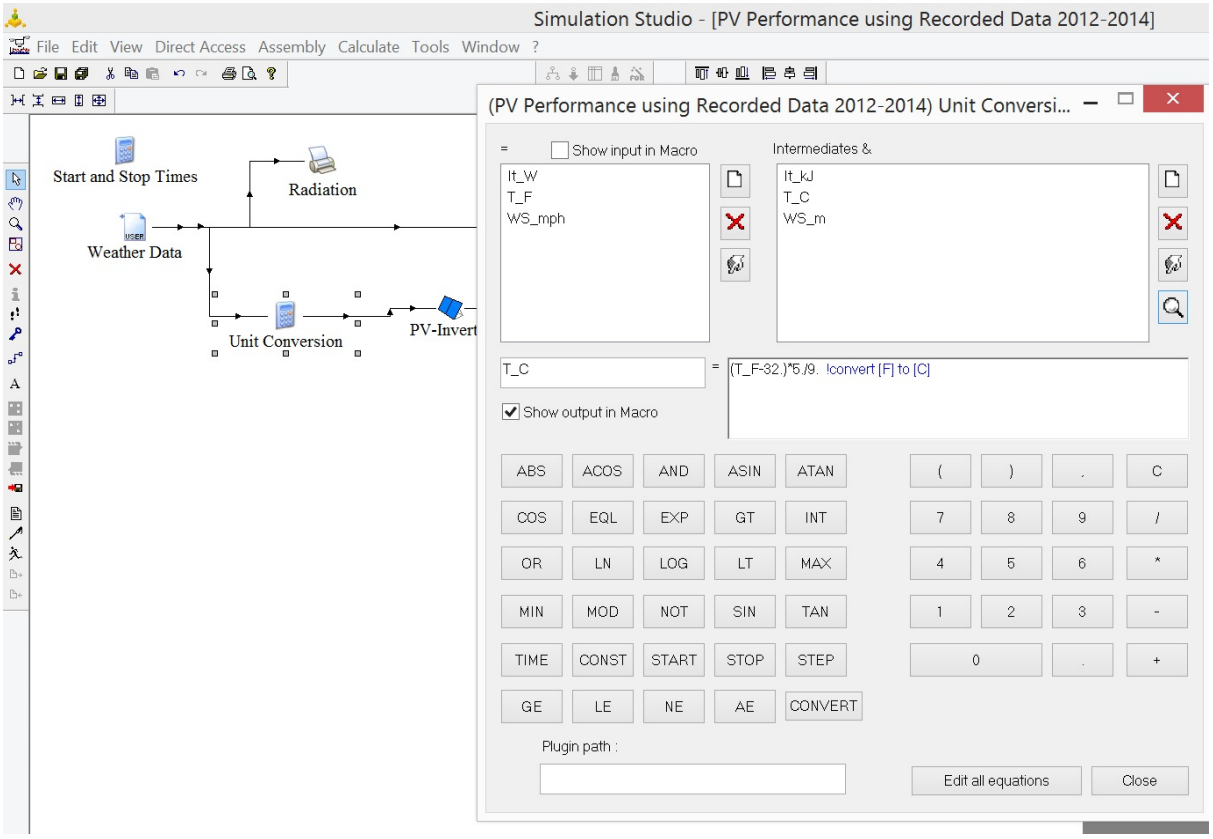

Figure D - 5. Controller 2 conversion to SI units.

    b. Figure D - 6 shows the connections between the outputs of Controller 2 into the inputs of Type194b (labeled PV-Inverter).

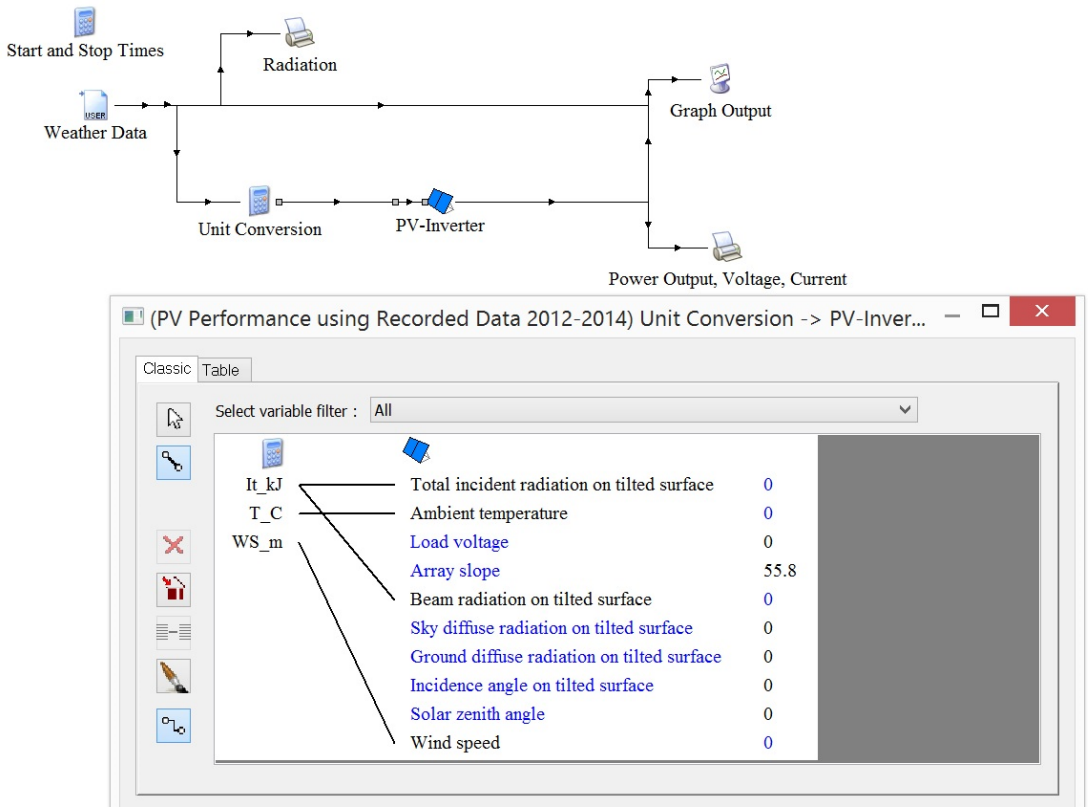

Figure D - 6. Connections between Controller 2 and Type194b.

5. Type194b is the component that uses the five parameter model to calculate power performance. Figure D - 7 shows the parameter window for this component.

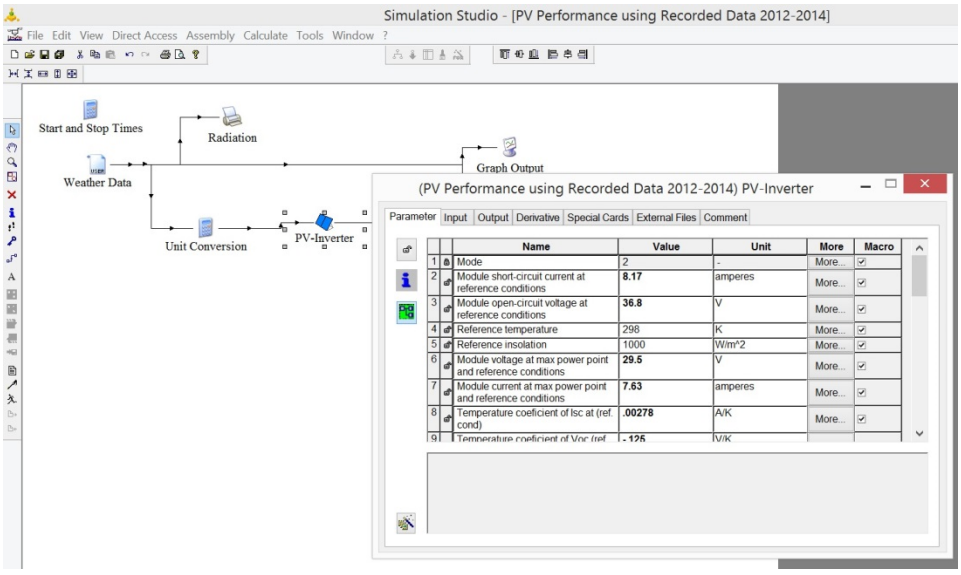

Figure D - 7. Type194b parameter window.

a. The parameters from the manufacturer data sheet are input into parameters 1 – 10 and 13 – 15.

b. Information about the solar panels (ex. how many wired in series) are input into parameters 11, 12 and 16.

c. The inverter information is input into parameters 25 – 27.

d. Figure D - 8 shows the connections between the outputs of Type194b into the inputs of the graphing component Type65d (labeled “Graph Output”).

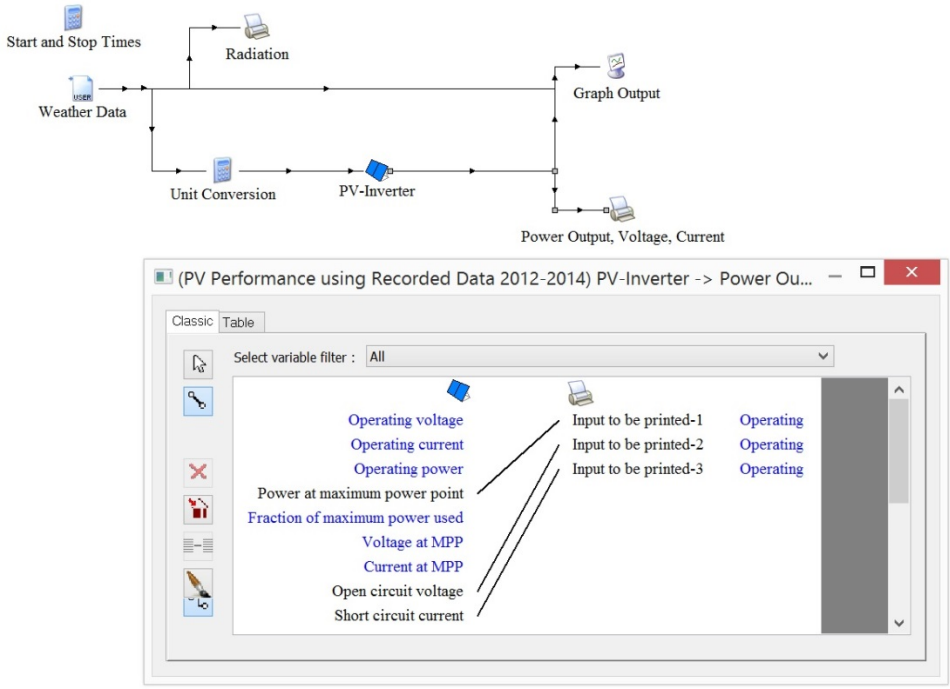

Figure D - 8. Connections between Type194b output and Type65d input.